Value of MRI preoperatively in guiding therapy of biopsy proven breast cancer

Sandra Stijven

promotor :
Prof. dr. Marie VANDERSTEEN ,
dr. L. MEYLAERTS

co-promotor :
Drs. Ellen GIELEN

Eindverhandeling voorgedragen tot het bekomen van de graad master in de biomedische wetenschappen klinische moleculaire wetenschappen

Maastricht University

universiteit hasselt

Senior practical training

Value of MRI preoperatively in guiding therapy of biopsy proven breast cancer

Sandra Stijven
0421891
2nd master Clinical Molecular Sciences
Senior practical training 2008-2009
University of Hasselt, Diepenbeek
Ziekenhuis Oost-Limburg, Genk
Department of Radiology
Supervisors: Dr. L. Meylaerts, Dr.Sc. E. Gielen, Dr. M. Horvath,
Prof. Dr. M. Vandersteen, Prof. Dr. L. Vanormelingen

Content

Acknowledgements

Five years ago, I started to study biomedical sciences. During these years I have grown a lot in the world of life sciences and also as a human being. I would like to thank everyone who supported me and made it possible for me to become a biomedical scientist.

First I want to thank everyone from the University of Hasselt for teaching and helping me during these five years. I also want to thank everyone who helped me during my research of the last eight months. I will thank Prof. Dr. Y. Palmers for giving me the chance to work in the department of Radiology. I will also thank Dr. J. Vandevenne and Dr. L. Meylaerts for giving me the opportunity to participate this interesting study and for guiding me in the study, and Dr. M. Horvath who also learned me more about breast imaging. Lots of thanks to Dr.Sc. E. Gielen who guided me, supported me and gave me a helping hand during this research. Thanks to the gynaecologists Dr. J. Vlasselaer, Dr. G. Van de Putte and Prof. Dr. E. De Jonge for participation and planning of the MRI examinations. I will also thank Dr. J. Van Robays for his interest in this topic and his willingness to guide me in the world of breast pathology. Finally I will thank my intern promoters Prof. Dr. L. Vanormelingen and Prof. Dr. M. Vandersteen for their interest and listening during this research.

Lastly, and most importantly, I want to thank my family, especially my parents who made it possible for me to start these studies and always supported me, believed me and helped me during difficult periods, like my brother, sister and other family members did. I also want to thank Tim who encouraged me during my final practical training. His love and confidence in me has taken the load off my shoulder.

Abbreviations

- **ADC**: apparent diffusion coefficient
- **B_0**: main magnetic field of the MRI scanner
- **BI-RADS**: breast imaging report and data system
- **BRCA**: breast cancer antigen
- **CA 15.3**: carcinogen antigen 15.3
- **CC**: cranio-caudal
- **CNB**: core needle biopsy
- **DCIS**: ductal carcinoma *in situ*
- **DWI**: diffusion weighted imaging
- **ER**: estrogen receptor
- **FNA**: fine needle aspiration
- **FOV**: field of view
- **Gd-DOTA**: gadolinium-tetraazacyclododecanetetraacetic acid (dotarem)
- **HER2**: human epidermal growth factor receptor 2
- **IDA**: invasive ductal carcinoma
- **ILA**: invasive lobular carcinoma
- **LCIS**: lobular carcinoma *in situ*
- **MLO**: medio-lateral oblique
- **MRI**: magnetic resonance imaging
- **NMV**: net magnetization factor
- **NOS** : not otherwise specified
- **NPI**: Nottingham prognostic index
- **PACS**: picture archiving and communication system
- **PD**: proton density
- **PR**: progesterone receptor
- **RF**: radiofrequency
- **ROI**: region of interest
- **STIR**: short TI (inversion time) inversion recovery
- **TDLU**: terminal duct lobular unit
- **TE**: echo time
- **TR**: repetition time
- **US**: ultrasonography

Abstract

Although magnetic resonance imaging (MRI) has a high sensitivity in the detection of tumours, there is still a lot of discussion about the role of this technique in breast cancer detection. Currently, the use of breast MRI is limited because of its high costs, its low to moderate specificity, the variability in image interpretation, and the variability in the use of parameters among institutions. As a result, MRI is not routinely used to further characterize lesions in patients diagnosed with breast cancer. The additional information of the cancer that can be acquired with a MRI scan may alter the staging of the disease, which can result in a change of the surgical plan. In this study, the impact of preoperative MRI on the surgical treatment of women with biopsy proven breast cancer was investigated. The diagnostic value of preoperative MRI was compared with that of conventional imaging. Simultaneously, the recently developed diffusion weighted imaging (DWI) technique was evaluated. 40 women were included in the study. All patients underwent conventional imaging (mammography and ultrasonography (US)) and biopsy as part of the clinical workup. In addition, preoperative MRI was performed in each patient. The kinetics of contrast captation was monitored and apparent diffusion coefficients (ADC) were calculated. All imaging findings were compared with the histopathologic results, which were used as the gold standard. Differences in tumour extent, as determined by US, MRI and histopathology, were evaluated. The results showed that the contrast captation kinetics curves are mostly aspecific, while there was a better concordance between tumour malignancy and ADC values. MRI revealed unsuspected multifocal and multicentric breast carcinoma in 20 patients (50%). With respect to defining the tumour extent, MRI correlated significantly better with histology than US. The surgical plan of 7 patients (18%) was changed as a result of the additional information provided by MRI.

1 Introduction

1.1 Breast cancer: definition and epidemiology

The development of breast cancer is the consequence of uncontrolled growth and division of the epithelial cells that line the terminal duct lobular unit (TDLU) [1]. Worldwide, breast cancer is the most common cancer among women. The risk of getting breast cancer in Western Europe is 60% greater than in Eastern Europe [2]. In 2001 and 2005, respectively 8118 and 9405 women were diagnosed with breast cancer in Belgium. The risk of being diagnosed with breast cancer still increases [3]. The geographical differences in breast cancer incidence and mortality in Europe in the year 2000 are shown in figure 1.

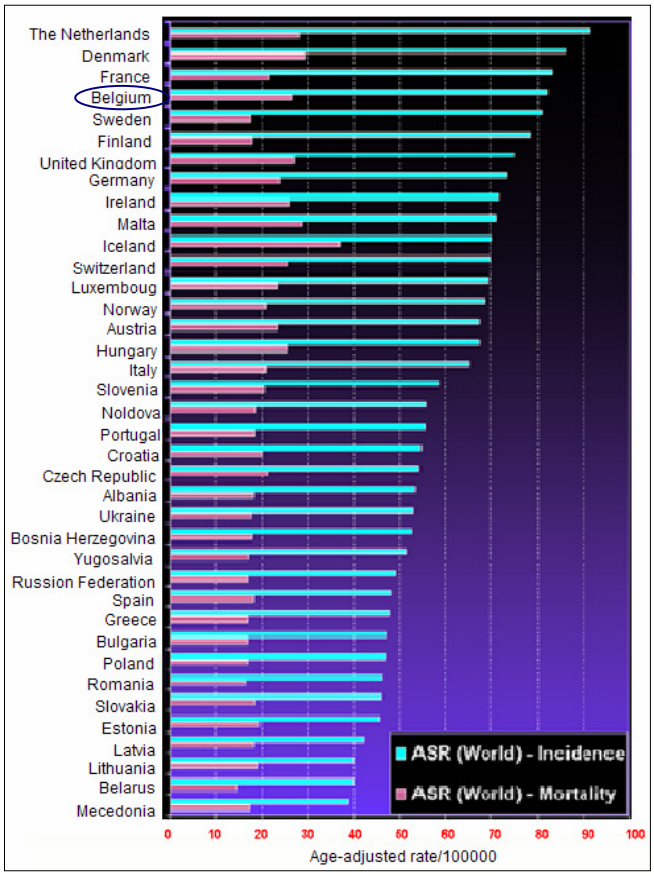

Figure 1: Breast cancer incidence and mortality in Europe, year 2000, by country (courtesy of [2]).

There are several risk factors that increase the chance of developing breast cancer. Genetics appears to be one of them. Women with one or two close relatives with breast cancer, have a three to four time times higher risk to develop the disease. The closer the cluster, the greater the effect; e.g. a woman with mother and sister affected is very likely to develop breast cancer, and at a younger than average age. Hereditary forms of breast cancer appear to be responsible for 8% of the disease. 80% of the familial breast cancers are related to mutations

in BRCA1 and BRCA2 genes. Women who inherit the BRCA1 gene have a 60% risk of developing breast cancer by age 50. About one third of women with hereditary breast cancer have mutations in the BRCA2 gene. BRCA genes act as tumour suppressor genes. Cancer arises when both alleles are inactive or defective, caused by a germ-line mutation and a somatic mutation. Mutation of BRCA genes result in a loss of tumour suppressor function. Other genes such as the HER2/NEU proto-oncogene and the tumour suppressor gene TP53 have also been identified as important players in the development of breast cancer [4,5]. Li-Fraumeni syndrome (linked to germline mutations of the TP53 gene), Cowden syndrome and Bannayan-Riley-Ruvalcaba syndrome (linked to germline mutations in PTEN gene) also increase the risk of developing breast cancer [6].

Another important risk factor is age. Breast cancer is less common in women younger than age 30 and increases throughout life. This increase almost stops after the menopause [5]. Figure 2 illustrates the age-specific incidence of breast cancer in Belgium in 2001 and 2005.

Hormonal influence, such as an excess of estrogens, also plays a significant role in the development of breast cancer. Estrogens stimulate the production of growth factors by normal breast epithelial cells and by cancer cells. A prolonged exposure to estrogens, as occurs in women having an early menarche or late menopause, may increase the risk of developing breast cancer [5]. Since fat cells produce estrogens, obesity is also a risk factor. The risk of breast cancer increases with age at which a women bears her first child. Although the exact reason for this is still unknown, it appears that pregnancy produces certain changes in the hormonal environment. Estriol, produced during pregnancy, may be protective against the cancer inducing effects of estrogens [4].

Another risk factor for breast cancer is ionizing radiation, more exactly the radiation dose, the exposure time and the age of exposure. Radiation is more detrimental during breast development [5]. Since mammography uses low doses of radiation, the possible hazard from mammography x-rays is low. Above age 50, mammography is highly beneficial, especially for women who are at high risk of developing breast cancer [7]. Other, less well-established risk factors for breast cancer are smoking and alcoholic consumption [5].

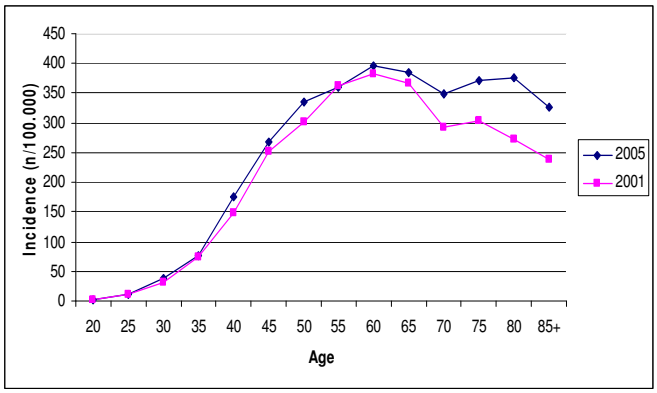

Figure 2: Age-specific incidence of breast cancer in Belgium, 2001 and 2005. The incidence increases slowly from the age of 20, than sharply increases from 40 to 60 years and is the highest at age 60 [3].

1.2 Anatomy of the breast

The mammary gland lays on the pectoralis muscle of the chest wall. It consists of fat, fibrous connective tissue and glandular tissue, and is encased by skin. There are three visible anatomical portions (figure 3A); the gland itself, the mammary papilla (nipple) and the areola (darker pigmented area around the nipple). The mammary gland contains 15 to 20 lobes with varying numbers of ducts and lobules [8]. The ducts and lobules, together with the interlobular fibrous tissue, are commonly referred to as the breast parenchyma. This parenchyma is diffusely distributed within the fatty tissue of the breast [9]. The lobules are clusters of alveoli and are responsible for the production of milk. Each lobe is drained by a lactiferous duct that opens in the nipple. Each duct has a dilatation close to the apex of the papilla, which is called the lactiferous sinus [8]. The lobule, together with its terminal duct, has been called the terminal duct lobular unit (TDLU) (figure 3B) [10]. The ducts consist of an inner cylindrical epithelium, outer myo-epithelial cells and a basement membrane. Alveoli are lined by cuboidal to columnar epithelium and an outer myo-epithelial cell layer. The major blood supply of the breast comes from the lateral thoracic and internal thoracic arteries. The breast is innervated by intercostal nerves that carry both sensory and autonomic fibers. 75% of the lymphatic drainage involves axillary pathways [8].

In clinic, the breast is viewed as the face of a clock with the patient facing the observer. Quadrants and the letters ABC are used to describe locations of lesions within the breast; A is the position close to the nipple and C is the position at the periphery (appendix 1). When a lesion is found, its three-dimensional location within the breast must be known. The depth of a lesion can be described as anterior, posterior, cranial or caudal [11].

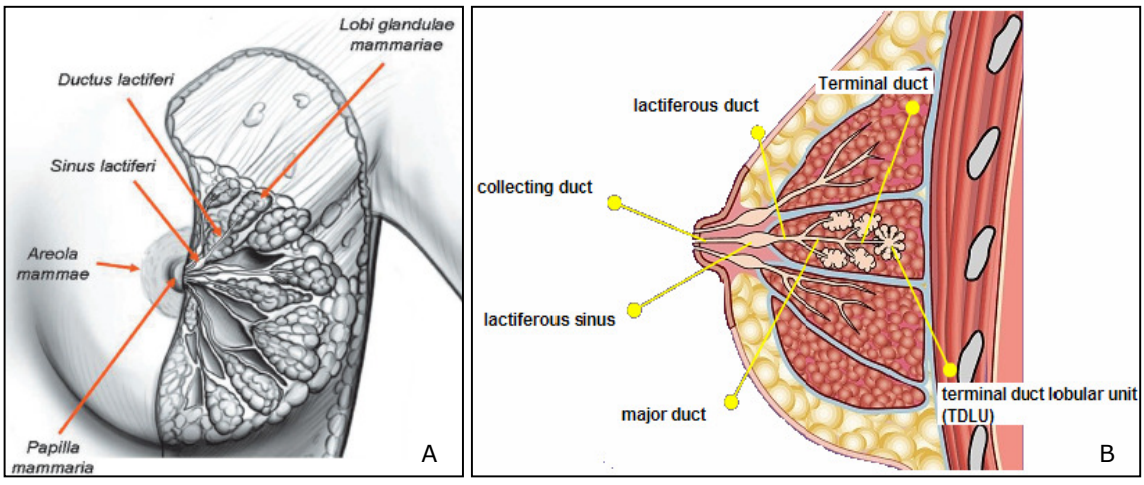

Figure 3: (A) Anatomy of the left breast (courtesy of [12]). (B) The deepest point of the ductal tree of the mammary gland, the TDLU, is the point mostly affected by pathologic changes, i.e. this is where most carcinomas or benign proliferative lesions develop (courtesy of [13]).

1.3 Pathology

Most pathologic lesions inside the breast arise from the TDLU [10]. The components of the TDLU undergo alterations at time of pregnancy and during women's regular monthly menstrual cycles. These cyclic changes in the breast involve the specialized stromal components as well as the epithelial cells of the lobular unit. Fibrocystic changes (also called mammary dysplasia) is a common benign entity. The term may be synonymous with increased breast lumpiness and pain in the second half of the menstrual cycle. Fibrocystic changes can be due to hormonal imbalance, particular estrogen excess. The morphologic findings may be simple cysts or may result in sclerosing processes resulting in the formation of radial scars which may be mistaken for carcinomas. The histologic features of fibrocystic changes are complicated by a subset of epithelial proliferative changes in the TDLU. An increase in the number of cells lining the terminal ductules is also called ductal epithelial hyperplasia. Another form of hyperplasia also involves the cells lining the terminal ducts, but it has a different histologic and cytologic appearance, and is termed lobular hyperplasia [9].
Epithelial hyperplasia may be one of the first steps in the development of breast carcinoma [1]. There appears to be a morphologic spectrum that extends from minor degrees of hyperplasia, throughout exuberant- but cytologically benign- hyperplasia, to cytologic atypia and other cytologic features characterized as carcinoma *in situ* to invasive carcinoma (figure 4). When some, but not all, of the features of malignancy are present in these proliferating lesions, the diagnosis of "atypical" ductal or lobular hyperplasia is made. The atypical proliferative lesions increase the risk for the subsequent development of carcinoma of the breast approximately four to five times that of the general population. Such a lesion is a purely microscopic finding that can be recognized as abnormal and likely to have malignant potential. Atypical hyperplasia is considered a pre-cancerous condition [9,1].

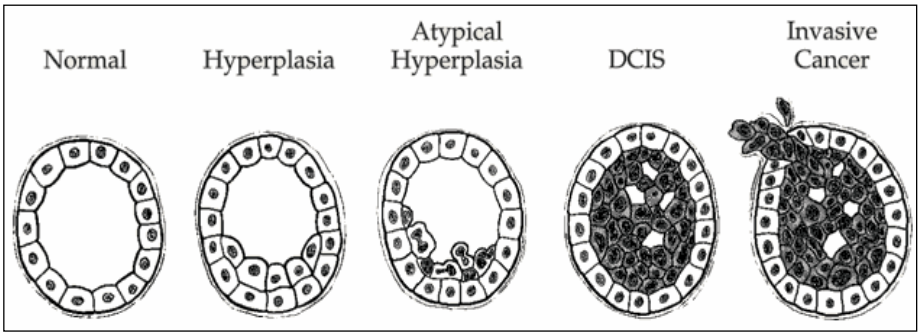

Figure 4: Breast cancer development (courtesy of [14]). DCIS: ductal carcinoma *in situ*.

The most common benign neoplasm of the breast is the fibroadenoma. Fibroadenoma is a benign tumour that originates from the TDLU. It is composed of a mixture of fibrous connective tissue and epithelial ductal structures. It is generally assumed that fibroadenoma results from an abnormal sensitivity to estrogens in the breast. Fibroadenomas commonly

enlarge under the influence of pregnancy and regress after the menopause. Other benign neoplasms of fat, blood vessels, or other connective tissue components may also be found in the breast [9].

Carcinoma, or breast cancer, is most common within the upper outer quadrant of the breast. Breast cancers can be divided into non-invasive and invasive cancers. Non-invasive cancers have not penetrated the basement membrane and do not invade into stroma or lymphovascular channels. Invasive (infiltrating) cancers have penetrated the basement membrane. There are two types of non-invasive breast cancers, namely ductal carcinoma *in situ* (DCIS) and lobular carcinoma *in situ* (LCIS) [5]. DCIS and LCIS arise in the TDLU, and there is frequent admixture of these two subtypes [9,1]. Comedo-carcinoma is a form of intraductal carcinoma. A hallmark of this carcinoma is necrosis of the tumour cells. Necrotic debris results in microcalcifications which are radiographically detectable [9]. The majority of cases of DCIS are detected as asymptomatic microcalcifications or architectural distortions on mammography. Some DCIS may present clinically with a mass, nipple discharge, or nipple eczema. LCIS is mostly an incidental finding, it does not form masses and it is rarely associated with microcalcifications. The presence of LCIS carries a 10-fold increased risk of developing invasive breast cancer [1].

The most important types of invasive breast cancers are invasive ductal carcinoma (IDA) and invasive lobular carcinoma (ILA). Invasive ductal carcinomas are also called "not otherwise specified (NOS)", because they cannot be classified into specialised types and they do not specifically arise from the ductal system [5]. IDA is the most common invasive breast carcinoma (60%-80%). It is usually associated with DCIS. ILA is the second most common type of invasive breast carcinoma and accounts for approximately 10% of all invasive breast malignancies. ILA infiltrates the fatty tissue in a very characteristic way with one cell behind the other in the so-called "Indian" filing pattern [1]. ILA is usually associated with LCIS. Other less common invasive cancers are medullary carcinoma, colloid carcinoma, tubular carcinoma, and inflammatory breast cancer.

Malignant cancer cells can spread into the breast tissue, blood and lymphatic vessels and travel to distant sites. Metastasis is the appearance of a mass of cancer in another part of the body at a distance from the original cancer [5]. Human tumours tend to spread first to regional lymph nodes and permeate the small capillaries and lymphatics in the breast parenchyma. The main sites of distant spread include the lungs, liver, and brain but adrenal gland and bones are also at risk [1].

1.4 Diagnosis of breast cancer

There are three important methods to diagnose breast cancer: clinical breast examination (palpation), medical imaging and histopathology (biopsy). Medical imaging includes mammography, US and MRI (see section 1.6).

1.4.1 Clinical breast examination

Clinical breast examination or breast self-examination is the first important stage in breast cancer screening. Breast awareness means that women have to be aware of changes of the breast tissue, like the size of the breasts, a persistent nodularity, pain and nipple contraction. Breast tissue undergoes changes each month during the menstrual cycle. Therefore, the best time to perform breast self-examination is about a week after the start of a period when the breasts are least likely to be swollen and sensitive [4,11].

1.4.2 Mammography

A mammogram is an x-ray examination of the breast. It is still the primary imaging modality used for breast cancer screening and diagnosis. Mammograms can be performed on women with signs and symptoms of breast disease. This is called diagnostic mammography. Mammography of asymptomatic patients for the purpose of screening for breast cancer is called screening mammography. Mammography uses x-rays at low kilo voltages to differentiate between fatty and soft fibroglandular components of the breast. It can depict lesions that are clinically occult and is used to screen both breasts. Mammography allows the detection of microcalcifications, which may be the first indicators of malignant breast disease. The presence of malign-appearing calcifications in a mass that appears otherwise benign is an indicator for biopsy, as microcalcifications are associated with about 30% of the invasive breast cancers. Suspected breast lesions may appear as a dense area, as architectural parenchymal distortion, or both on the image [4,11,15]. It is worthwhile to note that the differences in the ratio of parenchymal to fatty tissue have important implications with respect to the radiologic evaluation of breast disease. In woman with abundant mammary fibrous tissue, the breasts are more difficult to evaluate by mammography than in woman whose breasts are predominantly fatty. The term mammary dysplasia is commonly used to describe radiographic dense breasts [9].

The sensitivity of mammography depends on tumour size and breast density [16]. In general, mammography has a sensitivity of about 78%, while in dense breasts this is 44% [17]. The sensitivity is high in fatty tissue but decreases in dense breast tissue (a high proportion of fibroglandular tissue). Since the glandular breast tissue is sensitive to radiation, asymptomatic

women without risk factors should not undergo mammographic screening before the age of 40 years. Since radiation exposure may increase the risk of developing breast cancer, a radiation dose as low as reasonably achievable (ALARA principle) is used in order to produce an image of acceptable diagnostic quality [4]. Higher-energy radiation, however, is required in dense breast tissue and in large breasts. In order to obtain a mammogram of good quality, the breast needs to be compressed. The compression mobilizes the breast and decreases the thickness of the breast. In this way the x-ray beam penetrates more uniformly, allowing a lower radiation dose. In addition, compression reduces scattered radiation and thus improves contrast. Furthermore, breast compression spreads the normal tissue while malignant foci persist. Small areas of pathology which are hidden in the glandular tissue can thus be visualised, and architectural distortion can be depicted [4,11,15].

1.4.3 Ultrasonography

US is used as an additional evaluation of mammographic and palpable abnormalities and has become a invaluable problem-solving tool when mammography is inconclusive. It may improve the specificity of mammography in characterizing masses. With the combination of a negative mammogram and a negative sonogram, the likelihood of malignancy has been shown to be less than 3%. In a study of lord et al., mammography alone depicted only 25-59% of breast cancers whereas mammography and sonography together depicted 49-67% breast cancers [18]. Sonography may be used as a screening tool for young women who are at high risk to develop breast cancer. These women have more dense breast tissue, which makes mammography less sensitive. Sonography is good in diagnosing cysts, eliminating the need for biopsy of these benign masses. Most carcinomas are seen on a sonogram as hypo-echoic masses. Distortion seen on US should be followed by biopsy [11,15].

1.4.4 Biopsy

Irrespective of the imaging techniques used, biopsy is always required for a definitive diagnosis when a suspected malignant mass or calcifications are depicted. An advantage of biopsy is the prevention of unnecessary operations. Due to the small volume of tissue removed, there are no cosmetically deforming scars that might impair the interpretation of subsequent diagnostic images [19]. Guidance for percutaneous biopsy is provided by stereotaxis, ultrasound, and more recently by MRI. Virtually any breast lesion that is seen on US can be sampled with a needle under sonographic guidance [20]. Both fine needle aspiration (FNA) and core needle biopsy (CNB) are effectively guided by real-time sonography. Fine needle aspiration is accurate and minimally invasive. It can confirm (or rule out) metastatic involvement of lymph nodes. Core needle biopsy allows a histological diagnosis of larger tissue samples. It can assess the invasiveness of a cancer [19]. Stereotactic breast biopsy is an x-

ray guided method for localizing and sampling breast lesions discovered on mammography, but not seen by US [21]. MRI guidance is used to calculate the position of abnormal masses only seen on the magnetic resonance image, to verify the placement of the needle. The patient lies in prone position on a table and with the help of computer software the position of the lesion and the position and depth of the needle is calculated [22].

1.5 Treatment of breast cancer

In the past, radical mastectomy was the only surgical treatment for breast cancer. Currently, modified radical mastectomy or breast-conservation therapy is preferred. Modified radical mastectomy includes the removal of the whole breast, a partial axillary dissection, but spares the pectoralis major muscle. Breast-conservation therapy, also called lumpectomy, only removes the tumour with a margin of the surrounding tissue. Complete excision of the tumour is required in order to reduce local recurrence as much as possible. [4,15]. About a third of all breast cancers are unsuitable for breast conservation surgery (e.g. too large, multifocal lesions,…), and some patients who are suitable for this kind of treatment opt for mastectomy. When the tumour is too small to be detected during the operation, an image guided tracking is usually performed. This technique uses sonography or mammography as a guide to visualize the lesion and to place a wire in order to direct the surgeon toward the tumour [23].

During surgery, a sentinel node procedure is performed to check the axillary lymph node status. The sentinel node is the first draining node on the direct drainage pathway from the primary tumour site. If the sentinel node contains cancer, there is a 40% risk that higher order nodes may also be affected. The sentinel node is visualised by injecting the patient with a radioactive dye. Immediately after the removal of the sentinel node, which takes place during the breast surgery, histopathologic evaluation is performed. In case of a positive result, a total axillary dissection is performed [24].

The postoperative treatment of breast cancer depends on histological findings. Radiation therapy is generally recommended for all women who received breast conservation surgery and in women who received mastectomy with high probability of recurrence. Radiation therapy is usually combined with chemotherapy, which inhibits the cell growth of possible residual tumour cells. Chemotherapy can also be used preoperatively to reduce the tumour size, if it is too large to perform a surgery. This is also called neoadjuvant chemotherapy [25]. Approximately 50-70% of breast cancers require estrogens to grow. Hormonal therapy can be used when a cancer is estrogen receptor-positive or progesterone receptor-positive. An example of an anti-estrogenic drug is Tamoxifen. When the HER2 receptor is overexpressed, the antibody Herceptin (Trastuzumab) can be used to block the growth of possible residual tumour cells [4,15].

1.6 Magnetic Resonance Imaging (MRI)

1.6.1 Basic principles

Magnetic resonance imaging (MRI) is a non-invasive imaging technique that uses sound waves and magnetic fields to obtain detailed information of the soft tissues in the human body. The technique relies on the magnetic characteristics of the nuclei of hydrogen atoms, the most abundant atom in the human body. Hydrogen atoms can take up and emit radiofrequency energy packages. Each hydrogen nucleus contains a single proton with a positive charge that continuously spins (moves) around its axis. As a result, the hydrogen nucleus has a magnetic field and acts as a small magnet. The magnet of each nucleus has a north and a south pole. The north/south axis is called the magnetic moment. In the absence of an applied magnetic field, these magnetic moments are randomly oriented in the human body, resulting in a net magnetic field of zero (figure 5A).

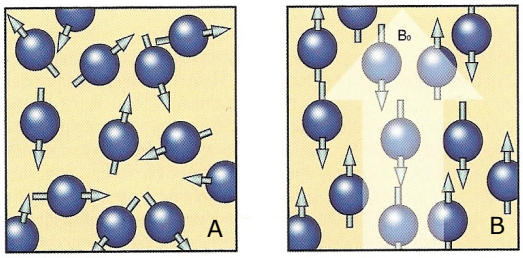

Figure 5: (A) random alignment, no external field. (B) Alignment due to external magnetic field (courtesy of [26]).

The MRI scanner consists of a tunnel (i.e. the bore) with a strong magnet that generates a magnetic field (B_0). The patient lies on a table, which is moved inside the bore and is exposed to a horizontal magnetic field (z-direction from toe to head). The magnetic field strength varies between 1.5 and 3 Tesla in medical practice. B_0 induces the magnetic moments of the hydrogen atoms to align in two possible directions with regard to the magnetic field (figure 5B). Magnetic moments can align in the same direction as B_0 (parallel or spin-up) or in the opposite direction (anti-parallel or spin-down). There is always a larger number of magnetic moments that align in the same direction as B_0 as this costs less energy. The result is a net magnetic moment, parallel with B_0, which is represented by a net magnetization vector (NMV) (figure 6). This is also called longitudinal magnetisation.

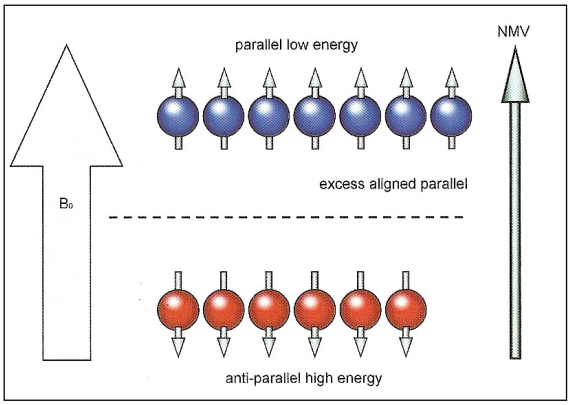

Figure 6: The net magnetization factor (NMV) (courtesy of [26]).

Each hydrogen nucleus is spinning around its axis. The influence of B_0 produces an additional spin, or wobble of the magnetic moment of the hydrogen atom around B_0. This secondary spin is called precession and causes the magnetic moments to follow a circular path around B_0. The speed at which they wobble around B_0 is called the precessional frequency or Larmor frequency. The value of the precessional frequency is governed by the Larmor equation, which states that:

$$\omega_0 = B_0 \times \lambda$$

where ω_0 is the precessional frequency, B_0 is the magnetic field strength of the magnet and λ is the gyro-magnetic ratio. All MR active nuclei have their own λ (e.g. the gyro-magnetic ratio of hydrogen is 42.57 MHz/T) so that they precess at different frequencies when they are exposed to the same field strength. This allows specific imaging of hydrogen while ignoring other magnetic resonance active nuclei in the body.

In addition to the magnetic field B_0, the MRI scanner generates radiofrequency (RF) pulses in a direction perpendicular to B_0. The nucleus gains energy and resonates if the RF pulse of energy is exactly the same as the Larmor frequency of the nucleus. Other MR active nuclei that have aligned with B_0 will not resonate, because the energy is delivered at a different frequency to that of their precessional frequencies. The application of an RF pulse that causes resonance to occur is termed excitation. The absorption of energy causes an increase in the number of spin-down hydrogen nuclei, because some of the spin-up nuclei gain energy and become high-energy nuclei. As a result, the NMV moves out of alignment, away from B_0, to the transverse plane. The angle to which the NMV moves out of alignment is called the flip angle.
When the RF pulses are turned off, the hydrogen nuclei lose the energy that they had taken up from the RF pulse and the NMV realigns with B_0. This process is called relaxation and it can

occur in two different ways. T1 relaxation is also called longitudinal relaxation or spin lattice relaxation because the nuclei give their energy to the surrounding environment or lattice. The T1 relaxation time is lower (i.e. faster recovery) for more structured tissues. Fat is more structured than water and can easily absorb energy into its lattice. It thus has a relatively short T1 in contrast to free water, which has a long T1 (figure 7A). The larger the proportion of free water in a tissue, the longer its T1. T2 relaxation is also called transverse relaxation or spin-spin relaxation because the nuclei exchange their energy with neighbouring nuclei. The reduction of the transversal magnetization is dependent of the rate at which neighbouring nuclei move. The more rapid they move, the less rapid the transversal magnetization decreases. The more structured the tissue, the more quickly the T2 relaxation. T2 relaxation is short for structured tissue (fat) and long for free water. The greater the proportion of free water in a tissue, the longer its T2 (figure 7B).

During a MRI examination, the body part of interest is surrounded by receiver coils which will take up and measure the lost energy. If a receiver coil is placed in the area of the moving magnetic field, i.e. the magnetization precessing in the transverse plane, a voltage is induced in this receiver coil. This voltage constitutes the MR signal. The frequency of the signal equals the Larmor frequency, the magnitude depends on the amount of magnetization present in the transverse plane. The signal is processed and reconstructed to obtain 3D gray-scale MR images.

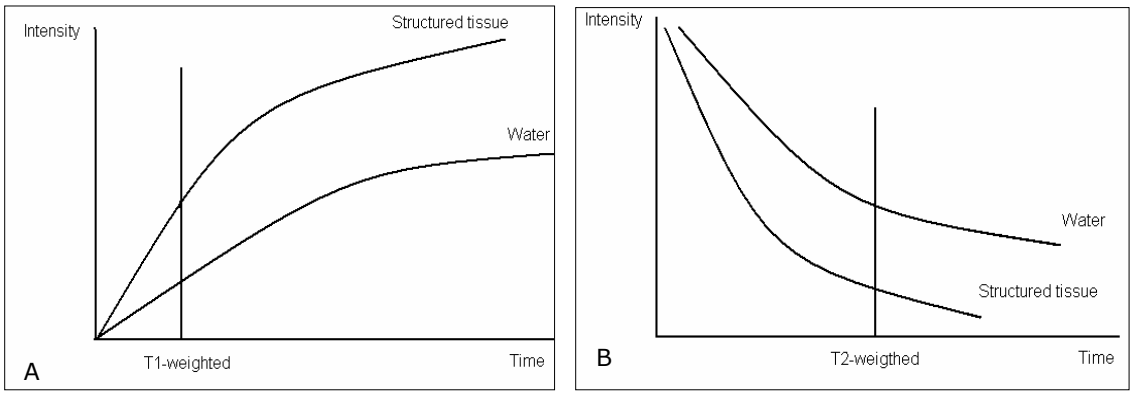

Figure 7: Water has a low intensity (dark) on a T1-weighted image (A) and a high intensity (bright) on a T2-weigthed image (B).

Image contrast depends on the mechanisms of T1 recovery and T2 decay, explained above, and proton density (PD). The two extremes of contrast in MRI are fat and water. The Larmor frequency of hydrogen in water is higher than that of hydrogen in fat. Hydrogen in fat recovers more rapidly along the longitudinal axis than hydrogen in water and loses transverse magnetization faster than in water. Subsequently, fat and water appear different on MR images. Abnormal tissue tends to have a higher PD, T1 and T2 than normal tissue, because of increased water content or vascularity. Image contrast is controlled by echo time (TE) and

repetition time (TR). These are selected to weight the contrast in an image. TR is the time from one RF pulse to the next RF pulse. It determines the amount of T1 relaxation between RF pulses. TE is the time from the RF pulse to the peak of the signal. It determines how much T2 relaxation has occurred. A deliberate choice of parameters can be made, with regard to the specific magnetic relaxation characteristics of water in the different tissues, to get selective images of the morphological structures that are examined in the human body. Contrast agents contribute to better disease detection and characterization by affecting T1 or T2 relaxation times of different tissues, inducing a contrast difference [26,27].

1.6.2 MRI of the breast

The angiogenic activity of tumours is the basic feature for breast cancer in detecting lesions on MRI. When breast cancers grow, they highly depend on oxygen and nutrients. The supply of oxygen and nutrients through normal vessels or through diffusion of the fibroglandular tissue, however, is not sufficient for the tumours to grow. This shortage increases when the tumour size expands. As a result, there will be hypoxic stress in the tumour cells. This effect stimulates the release of vascular endothelial growth factors that promote the formation of new vessels. This process is called angiogenesis. The new blood vessels help the tumours to maintain their metabolic homeostasis. The contrast agent that is used during a MRI examination can easily reach the highly vascularised tumour and disperses in the extravascular space due to the impaired quality of the neo-vessel wall. Images before the injection of contrast agent are subtracted form the images after contrast agent injection, which allows to visualise the regions containing a high amount of contrast agent. The highly vascularised tumour enhances on the magnetic resonance image and can be distinguished from the surrounding tissue. The kinetics of the contrast captation can be analysed. There is a correlation between the vessel density of a cancer and its enhancement pattern. But it is not only the vessel density that determines the enhancement. Other factors that contribute to the enhancement are the amount of contrast agent, the T1 contrast of the pulse sequence used, the baseline T1 relaxation time of different tissues, the efficacy of the contrast agent to shorten T1 relaxation time, and the diffusion rate of the contrast agent. Vessel wall roughness of tumours increases the presences of extracellular contrast [28].
Besides the high vascularisation, tumours are characterised by a high cellularity, which can be measured by DWI.

1.7 Aim of the study

Mammography remains the primary imaging modality for breast cancer screening. Mammography however suffers from limitations in the ability to detect cancer. This limitation is due to the obscuration of the tumour by superimposed fibroglandular tissue. The frequency of false-negative results is estimated to be 5-15%. Other traditional diagnostic tools, such as ultrasonography, are also known to have limitations in the diagnosis of breast cancer [29]. Only 20% to 30% of lesions suspicious for carcinoma on conventional mammography are, in fact, cancer on biopsy [4].

MRI has a high sensitivity (89-100%) for the detection of breast cancer [28]. It is able to detect additional breast lesions that are not visible on clinical breast examination, mammography and ultrasonography. In addition, MRI might give more information about the exact location, the precise size and the extent of the tumour as well as its multifocality or multicentricity. Furthermore, there is no concern of potential carcinogenesis due to x-rays [4]. Up till now, MRI of the breast is mainly used as a problem-solving tool, when conventional imaging methods show equivocal findings [28]. Other indications of using breast MRI is when the breast tissue is too dense, when the patient is at high risk for breast cancer, in order to evaluate neoadjuvant chemotherapy and to evaluate silicone breast implant integrity. An other important indication for performing breast MRI is preoperative staging of the cancer [30].
Accurate determination of the extent and possible multifocality of a tumour prior to surgery is essential. Underestimation of the tumour extent and missing of additional occult lesions by conventional imaging, may result in incomplete excisions, and thus the need for additional interventions. An important reason why preoperative breast MRI is not routinely used is that it is a very expensive procedure. Early and accurate detection of breast cancer might result in improved care, less additional interventions and thus reduced overall costs. The aim of this prospective study was to asses the impact of preoperative MRI on breast cancer diagnosis and treatment planning. In addition, DWI was evaluated.

2 Materials and methods

2.1 Patients

Between November 2008 and April 2009, 40 female patients were enrolled in the study. Demographic information and medical history were collected, as well as family and personal history of breast disease and other cancers, and the phase of menstrual cycle. It was also noted if patients smoke or have an allergy. Inclusion criteria were female patients with clinical, mammographic and sonographic findings that were highly suggestive for breast malignancy, and biopsy findings that proved breast cancer. These patients got a preoperative MRI scan. If an additional abnormality was diagnosed with MRI, US was immediately used to find the lesion and to perform an US-guided biopsy. Exclusion criteria were patients with a pacemaker, clips or other implanted devices that are not MRI compatible, obese patients, pregnant or nursing patients. Patients with a breast lesion not diagnosed as breast cancer were also excluded from the study.

2.2 Mammography and ultrasonography

Mammography was performed using a Siemens Mammomat 3000 Nova system. Both breasts were imaged in the craniocaudal (CC) and medio-lateral oblique (MLO) directions. On the MLO view, the lateral side of the breast is placed against the film holder. The x-ray beam penetrates the compressed breast from its medial to its lateral aspect. The CC projection is performed with the inferior part of the breast against the film. The x-ray beam transverses the compressed breast from superior to inferior. Structures that attenuate the x-ray beam more strongly appear whiter or denser on the film [4]. Once a mass was found, characteristics such as size, location, margin, density, presence of calcifications and presence of distortion were defined. Criteria of malignant lesions were irregular or ill delineated borders, spiculation, microlobulation and microcalcifications. Criteria of benign lesions were smooth and sharp borders, surrounding hypolucent rim and macrolobulation [11].

US was performed using a Siemens Acuson Antares system, which sends high frequency sound waves through the breast. The reflected waves are translated into an image. Criteria of malignant lesions were ill-defined or irregular margins, shadowing, hypoechogenicity without retro-acoustic shadow or heterogeneous echogenicity, tissue distortion and microlobulation. Criteria of benign lesions were hyperechogenicity, macrolobulation and capsule-like smooth borders [2]. The largest diameter of each lesion was measured.
Mammography and ultrasonography were scored on a 5-point scale, using the American College of radiology Breast Imaging Report and Data System (BI-RADS) (see section 2.5).

2.3 Biopsy

A percutaneous needle biopsy, either under stereotactic or US guidance, was performed in every lesion suggestive for malignancy based on conventional imaging techniques. US-guided fine-needle aspiration samples cells with a fine needle attached to a syringe after induction of local anesthesia. The needle content was transferred and fixed to a slide or injected into preservative for later cytological analysis. US-guided core needle biopsy uses a larger needle that is shot into the lesion with the help of a high-speed gun. A small incision has to be made in the skin. Stereotactic mammographic guidance can be used when the lesion is not visualized on ultrasound images. Stereotactic equipment is designed to calculate the position of a designated site within the breast by localizing its position in the x, y, and z axes from the breast surface [20].

2.4 MR imaging

Patients underwent a breast MRI examination after mammography, ultrasonography and biopsy. Bilateral MRI examinations were performed using a 1.5 Tesla scanner (Magnetom Symphony, a Tim System, Siemens medical, Erlangen, Germany). Patients were monitored during the scan by means of special equipment and communication with the patient could take place via an intercom.

Patients had to fill in a questionnaire (MR compatibility, medical history, body weight, …). Before the patient was positioned on the table of the scanner, an intravenous catheter was placed in an antecubital vein for later injection of intravenous contrast agent during the examination. The patient was positioned on a table in prone position, with the head towards the bore of the magnet (figure 8A). Images with high spatial resolution and good contrast were achieved with the help of designated coils. In case of breast MRI, both a breast coil (figure 8B) and a standard body coil were used. A breast coil yields better signal-to-noise ratio than a standard body coil. A correct positioning of the breasts in the breast coil is crucial for good quality examinations. The nipple should be as central as possible, and the breasts should not be compressed. A body matrix was placed on the back of the patient. The patient has to be installed as comfortable as possible (head phone, pillow to support the head, pillow underneath the lower legs) in order to prevent motion of the patient during the scan.

Dotarem® (gadoterate meglumine, Guerbet S.A., Paris, France) was used as contrast agent. Dotarem® (Gd-DOTA) is a Gadolinium-based substance, which shortens the T1-relaxation time of hydrogen, thereby increasing its signal intensity (positive contrast agent). The contrast agent was injected with a power injector at a rate of 2.0 ml/s, followed by a 20ml (1.0 ml/s) saline flush. The amount of contrast agent used depends on the body weight of the patient. In

this study, 1.5 dose of Dotarem® (0.15 mmol/kg corresponding to 0.3 ml/kg body weight) was used.

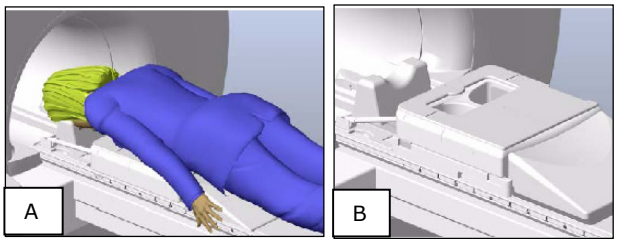

Figure 8: The patient lies in prone position on the table that moves into the tunnel (A). Breast coil (B).

2.4.1 Diffusion Weighted Imaging

DWI generates contrast by signal attenuation. The more restricted the diffusion of water molecules, the brighter the signal on DWI images. The apparent diffusion coefficient (ADC) values give an idea about the degree of diffusion. Normal tissue exhibits large signal loss (unrestricted fast diffusion) and has a high ADC value, while densely packed tumour cells show less signal loss (restricted slow diffusion) and appear bright on diffusion weighted images (low ADC value) [31]. The image intensities depend on the magnetic diffusion gradient (magnet strength), also called b-value (measured in s/mm^2). The higher the b-value, the stronger the DWI signal and the more precise evaluation of ADC values of the tumour. "Pure" diffusion contrast is obtained when using b-values above 1000 s/mm^2. However, image quality is diminished if large b-values are used. One should select a b-value that allows accurate evaluation of the tumour response on the one hand, and good image quality on the other hand [32]. By using different diffusion-weighted images obtained for different b-values, it is possible to calculate ADC maps, in which the T2-effect is filtered.

2.4.2 Imaging sequences

The MRI mammo protocol includes a localizer sequence, anatomical sequences and functional sequences. The localizer images are low-resolution template figures, used mainly for placing the slices in the right position and assuring that both breasts and axillary will be examined. A field of view (FOV) of 400 mm, slice thickness of 10 mm, TR of 20 ms, TE of 5 ms, a flip angle of 40°, and a voxel size of 3.1 x 1.6 x 10 mm were used. The acquisition time of the localizer images was 12 s.

The anatomical sequence applied after the localizer was a T2-weighted short TI inversion recovery (STIR) sequence (t2_tirm_tra_512_pat2) with the following imaging parameters: transversal orientation, acquisition time of 2 min 55 s, 30 slices, TR 6200 ms, TE 109 ms, TI 150 ms, flip angle of 150°, FOV 330 mm, voxel size 0.8 x 0.6 x 4.0 mm, and a slice thickness

of 4 mm. This sequence was used to reduce the signal from fat. Since water has a high signal on T2-weigthed images, these images were used to visualize fluid containing mostly benign lesions.

Diffusion weighted echo planar images (t2_epi_IR_trans_diffusion) were acquired to monitor the changes in the apparent diffusion coefficient (ADC) of lesions. 28 slices of 4 mm thickness were taken in the transversal plane, with the following parameters: TR 8100 ms, TE 83 ms, TI 180 ms, FOV 350 mm, voxel size 2.6 x 1.8 x 4 mm. The total acquisition time was 4 min 29 s. Consequently, an ADC map was generated using the following equation:

$$ADC = 1/b \times \ln (S0/S)$$

Where S0 and S are the signal intensities in the region of interest (ROI), respectively without and with diffusion weighting, obtained with different gradient factors (b values of 0, 300, 500 and 800 s/mm^2) [4].

Finally, a dynamic contrast-enhanced T1-weighted 3D fast low-angle shot pulse sequence (fl3d_tra_dyn_hires) was applied. The parameters of this sequence were: transversal orientation, 160 slices per set (a total of 1120 images), TR 4.39 ms, TE 1.66 ms, flip angle of 12°, FOV 400 mm, voxel size 0.9 x 0.8 x 1.0 mm, and a slice thickness of 1 mm. The acquisition time was 10 min 38 s. This dynamic sequence performs seven sets of measurements, with a total of 1120 images. The first series of T1-weighted images was acquired before the administration of contrast agent, the following six series were acquired after gadolinium was applied. The injection of contrast agent started simultaneously with the second set of dynamic images. When all images were collected, they were transferred to a workstation for post-processing.

2.4.3 Image post-processing

In order to visualize enhancing lesions, the pre-contrast image was subtracted from the second post-contrast image. All enhancing lesions were subsequently analysed by looking at the morphology, the kinetics of contrast captation, and by calculating the concordant ADC value. Morphology was analysed on the pre-contrast T1-weighted image as well as on the subtraction T1-weighted image. Lesions with irregular or spiculated borders were considered suspicious for malignancy. Lesion size was measured as the largest diameter of the enhancing region.

Kinetic analysis was performed by placing a ROI in the area of maximum enhancement of the lesion. Subsequently, a time-intensity curve was generated for that ROI. Three types of time-

intensity curves have been described: a linear curve, a plateau curve and a wash-out curve (figure 9). The first has a persistent increase in signal intensity after injection of contrast agent and would correlate with benign lesions (type 1). The second is a plateau curve which reaches a maximal signal intensity and then remains constant. It can correlate with benign or malignant lesions (type 2). The third curve correlates in most cases with malignant lesions (type 3) and shows a strong early enhancement in signal followed by a decrease in signal intensity over time (wash-out). Lesions showing a strong early enhancement and a wash-out effect are suspicious for malignancy. A slowly increasing poor enhancement was suggestive for benign lesions [33].

When a lesion was visualised on the subtraction image, it was identified in the corresponding slices of the diffusion weighted series. A ROI was drawn in the centre of the lesion on the b-800 DWI and subsequently copied to the ADC map in order to obtain the corresponding ADC value.

All processed images were archived to PACS (picture archiving and communication systems). PACS was used to archive and distribute digital images. Syngo Webspace allowed converting the images in 3D and in addition offered different tools to perform measurements. It allowed multidisciplinary consultation of the images, which could be viewed in all possible orientations.

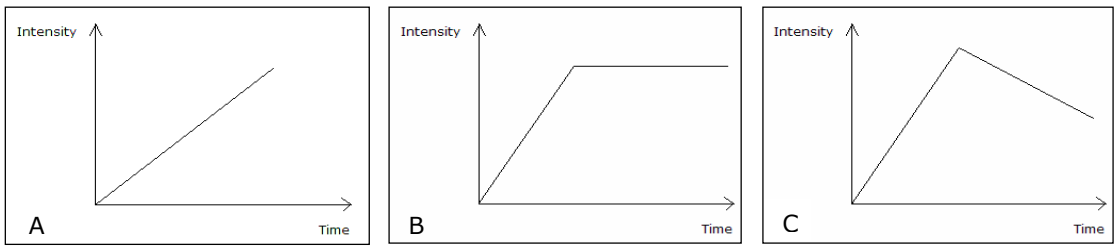

Figure 9: Three types of time-intensity curves. A: type 1, B: type 2, C: type 3.

2.5 Histology

Histopathological research of biopsy specimens was performed by an experienced breast pathologist. On pathologic examination, the diameter of each invasive and *in situ* cancer was measured. The BI-RADS of the American College of Radiology was used to define and categorize the lesions. Each lesion was characterised as benign (BI-RADS category 1, 2 or 3), suspected malignant (BI-RADS category 4 or 5) or known malignant (BI-RADS category 6). The TNM system was also used for tumour classification. T stands for tumour and determines the size of the tumour. N stands for nodes and determines lymph node invasion. M stands for metastasis and determines the cancer spread to other parts of the body. Immunohistochemistry was performed to predict the responsiveness of possibly residual

tumours to hormonal therapy. The hormone receptor status (estrogen receptor ER, progesterone receptor PR), the HER2/neu status, the Nottingham prognostic index (NPI), and the breast tumour marker CA 15.3 were assessed. The sentinel node was histologically evaluated to determine possible nodal metastasis.

2.6 Data analysis

MRI results were compared with conventional imaging to detect possible additional lesions that were occult at mammography and US. The tumour extent at conventional imaging and MRI was compared with the tumour extent at histology. Differences in tumour extent of 1 cm or more were defined as significant discrepancies, indicating underestimation or overestimation of the tumour size. Differences in tumour extent, as determined by US, MRI and histopathology, were evaluated using a paired t-test. The histopathology was used as the gold standard. Pearson's correlation coefficients were calculated to determine the associations between MRI, respectively US, measurements and the histopathologic tumour extent. Linear regression graphs were generated to present the relationship between the measurements of these two imaging techniques and the histopathologic size. The null hypothesis states that there is no correlation between the two variables. A p-value <0.05 was considered statistically significant and thus rejects the null hypothesis. Statistical values were calculated using XLSTAT and SigmaPlot statistical software, version 7.0. For each case an evaluation was performed to determine whether the MRI results had led to a change in the surgical treatment plan of the patient. MRI was assumed to have no effect on the treatment plan when similar results were obtained as those found at mammography, US and clinical examination. MRI changed the surgical management of the patient 1) if a wider excision was needed, 2) if additional lumpectomy was needed, or 3) when a mastectomy was performed instead of a breast conservation surgery.

3 Results

3.1 Patient population

Between November 2008 and May 2009, 144 patients got a MRI breast examination. 40 patients were enrolled in the study. These women had a biopsy proven breast cancer and underwent a preoperative MRI scan. The remaining 104 patients were excluded from the study because of various reasons (claustrophobia, obesity, check-up breast implants, postoperative follow-up, etc).

The age of the patients included in the study ranges from 29 to 83 years, with a mean age of 57 years. Histopathologic examination of the malignant lesions of these patients revealed 55% invasive and 45% mixed invasive/*in situ* cancers. 3 patients had multifocal and 16 patients had multicentric breast cancer. The remaining 21 patients had a solitary breast tumour. 70% of the patients found a palpable mass or pain in the breast, while in 30% of the patients the tumour was detected by screening. Mastectomy was performed in 32% and breast conservation therapy was performed in 50% of the patients. The remaining 18% of the patients were still receiving neoadjuvant therapy before the operation. Patient and tumour characteristics are outlined in appendix 2. The patients included in this study have biopsy proven breast cancer. The reason of performing biopsy was a positive mammogram and/or sonogram. Of all patients with breast cancer and with available mammographic and sonographic results, 5 patients had a negative mammogram but positive sonogram, 1 patient had a negative sonogram but positive mammogram. Of 4 out of 40 patients there was no mammographic information. Lymph node status could be determined in 32 of the 40 patients. Patients that were not included in this calculation underwent neoadjuvant chemotherapy or hormonal therapy before the operation. 38% of the patients had lymph node metastasis. The risk of lymph node metastasis increased when tumour size increased, when tumours were well-differentiated, and when there were multiple tumours in the breast (appendix 3).

3.2 MRI of the breast

MRI was performed after conventional imaging, biopsy and before surgery. MRI detected the tumour in all but 3 patients (8%). Besides these 3 false-negative results, there were 2 false-positive results. In 15 (38%) patients, MRI findings were comparable to those of conventional imaging.

3.2.1 Apparent diffusion coefficient

32 (80%) patients included in the study got echo planar imaging for diffusion weighting. The remaining patients did not get DWI since this technique was not yet routinely used in the beginning of the study. The ADC values of the malignant tumours ranged from 0.72 x 10^{-3} mm^2/s to 2.29 x 10^{-3} mm^2/s with a mean ADC value of 1.17 ± 0.36 x 10^{-3} mm^2/s. The ADC was also measured in 12 patients with benign lesions (1 patient of the study and 11 patients not included in the study). In benign tumours, the mean ADC was 1.58 ± 0.32 x 10^{-3} mm^2/s, varying from 1.17 x 10^{-3} mm^2/s to 2.10 x 10^{-3} mm^2/s (figure 10).

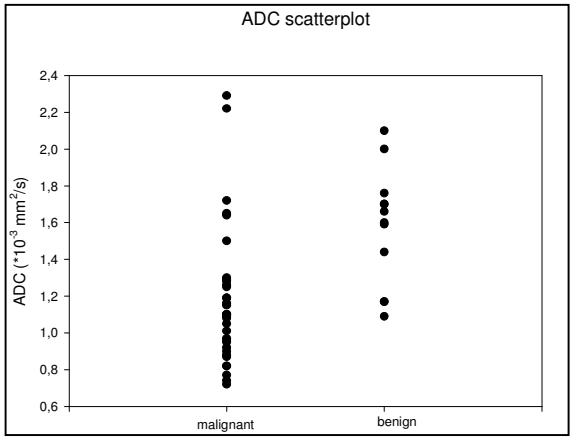

Figure 10: ADC values of malignant and benign lesions.

3.2.2 Contrast captation kinetics

Figures 11 and 12 show a benign, respectively a malignant breast tumour. The first case (not included in our study) is a patient with dysplasia (very dense breast tissue) on conventional imaging. For this reason an MRI examination was planned. MRI found an enhancing lesion of 5 mm in the left breast, which was classified as a benign fibroadenoma. This lesion has a smooth morphology, a continuous uptake of contrast (type 1 time-intensity curve) and a high ADC value of 2.10 x 10^{-3} mm^2/s. These are all characteristics of a benign lesion. The lesion was also seen on T2-weighted images, an additional feature in favour of benignity. Figure 12 shows the breast of a patient with a proven IDA. MRI showed a spiculated lesion, a wash-out curve type 3 and a low ADC value of 0.96 x 10^{-3} mm^2/s, all of which are characteristics of a carcinoma.

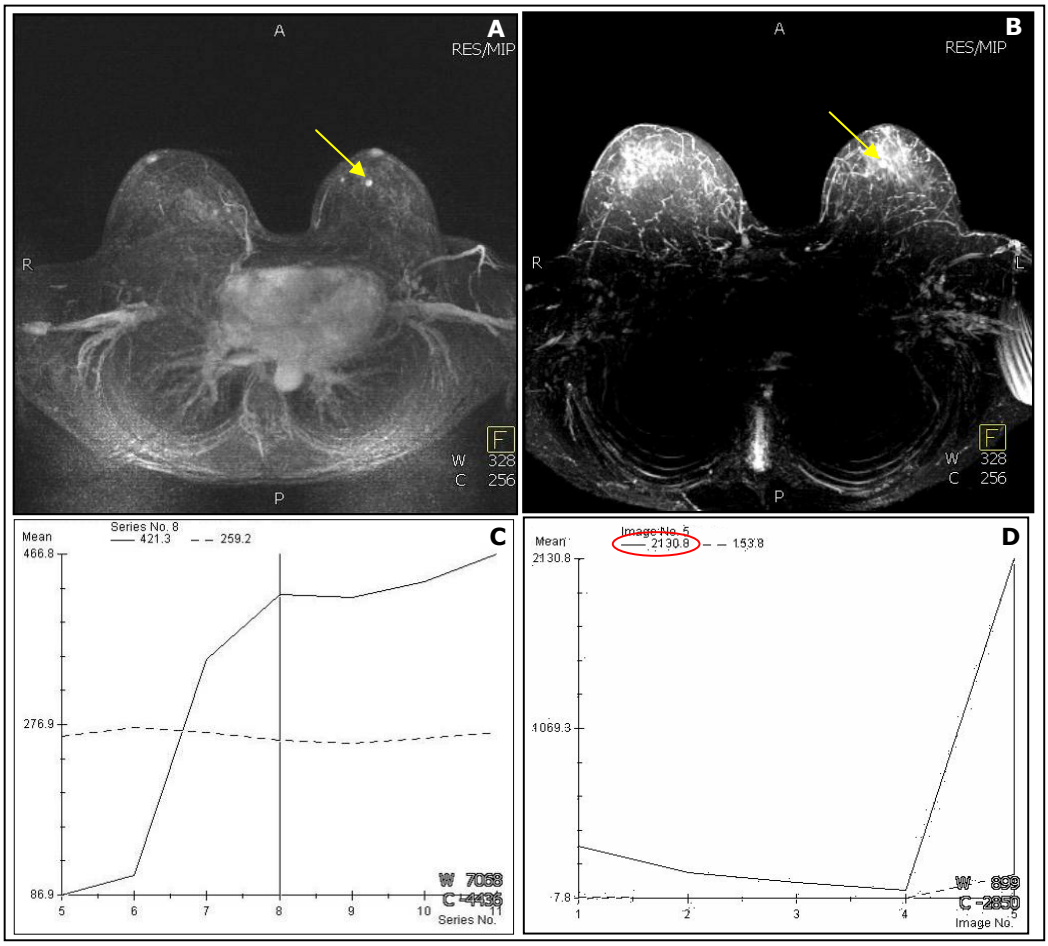

Figure 11: Patient with a benign lesion (fibroadenoma) in the left breast (yellow arrow), shown on the subtraction image (A). The lesion is visible as a hyperintense lesion on the T2-weigted image (yellow arrow) (B). The contrast captation curve of the lesion has a benign appearance (type 1), a persistent increase of signal intensity after contrast injection (C). DWI yields a high ADC value of 2.10 x 10^{-3} mm^2/s (D).

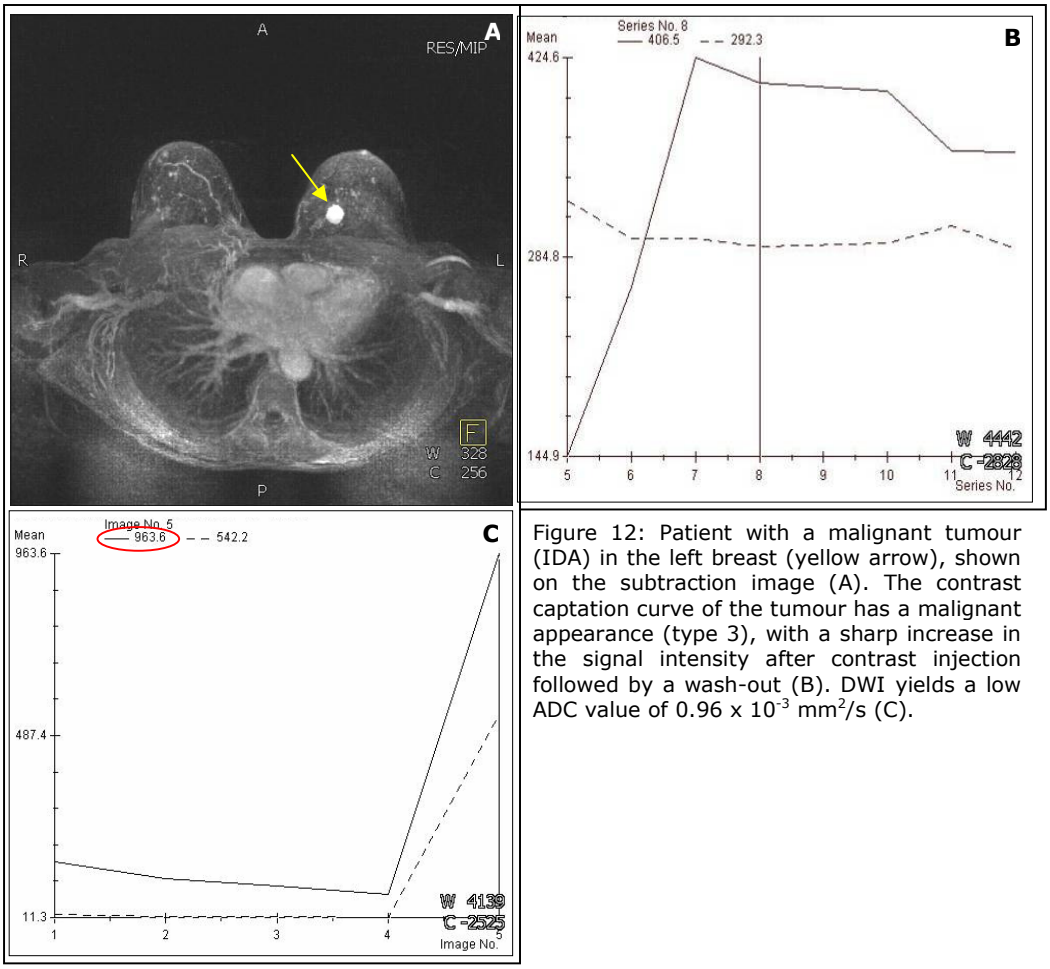

Figure 12: Patient with a malignant tumour (IDA) in the left breast (yellow arrow), shown on the subtraction image (A). The contrast captation curve of the tumour has a malignant appearance (type 3), with a sharp increase in the signal intensity after contrast injection followed by a wash-out (B). DWI yields a low ADC value of 0.96 x 10^{-3} mm^2/s (C).

The contrast captation kinetics (time-intensity curves) of the lesions were not always clear-cut in differentiating malignant versus benign lesions as is illustrated in figure 13. This patient had a biopsy proven malignant tumour (IDA). The tumour, which was found at conventional imaging, was also found as an enhancing lesions on the MR image. Despite the fact that this eye catching tumour is malignant (histopathologically proven), the time-intensity curve did not show persuading malignant characteristics and was inconclusive. However, the ADC of this lesion was low (1.1 x 10^{-3} mm^2/s), suggesting malignancy.

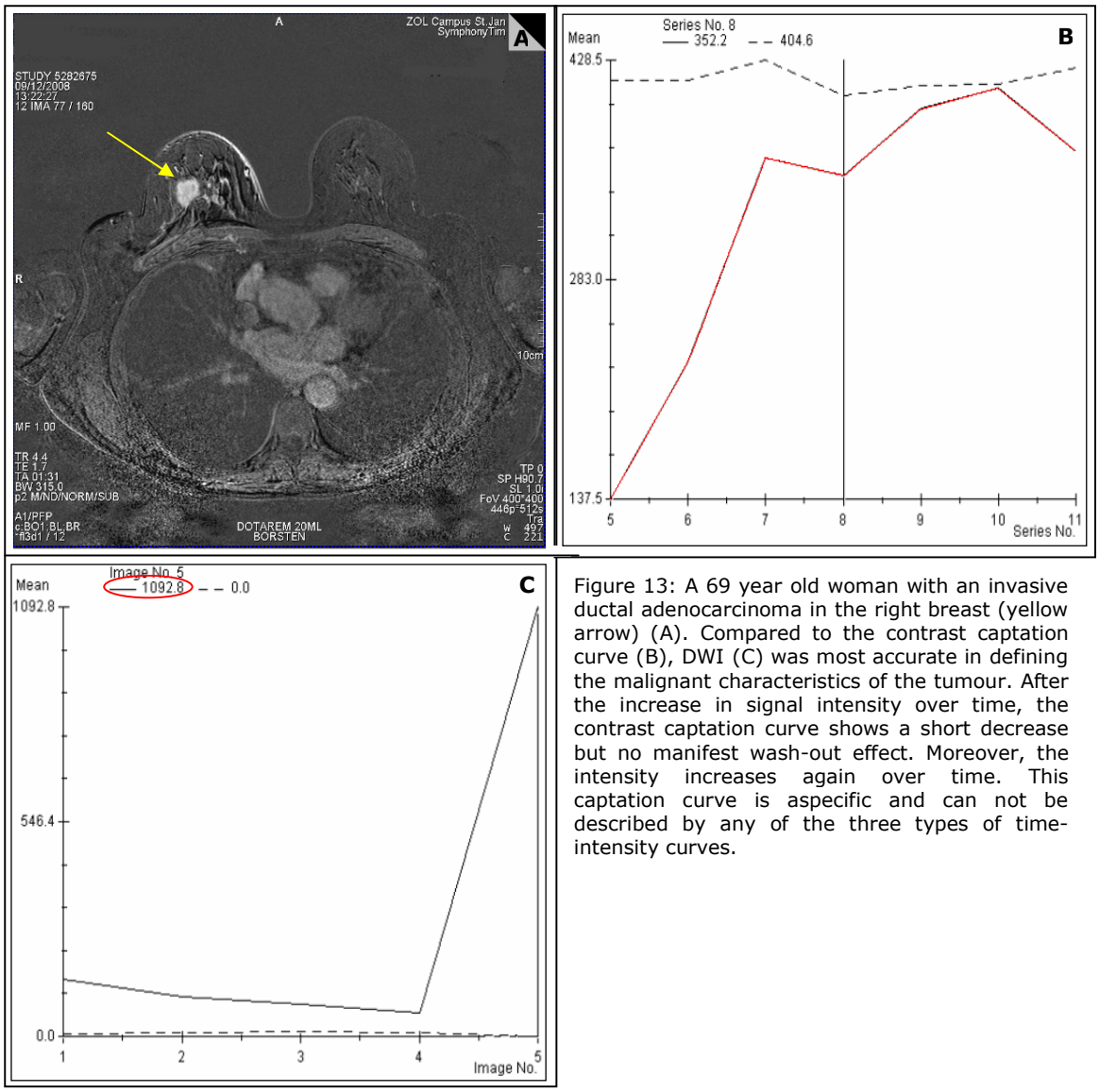

Figure 13: A 69 year old woman with an invasive ductal adenocarcinoma in the right breast (yellow arrow) (A). Compared to the contrast captation curve (B), DWI (C) was most accurate in defining the malignant characteristics of the tumour. After the increase in signal intensity over time, the contrast captation curve shows a short decrease but no manifest wash-out effect. Moreover, the intensity increases again over time. This captation curve is aspecific and can not be described by any of the three types of time-intensity curves.

3.2.3 Additional lesions

MRI depicted one or more additional tumours, not visible at conventional imaging, in 20 of the 40 patients (50%). In 3 of these 20 patients, MRI detected one or more occult multifocal lesions in addition to the known lesion (conventional imaging). In 16 of the 20 patients, MRI found multicentric tumours or could better define the extent of already proven multicentric tumours as additional small enhancing foci were identified. 3 patients had a hidden lesion in the contralateral breast. In one of them, the contralateral lesion could not be detected by US and therefore could not yet be classified as malignant . A follow-up MRI was planned after 6-8 weeks. In the other two patients MRI found additional multicentric lesions in the ipsilateral breast (2 of the 16 patients explained above), and an additional lesion in the contralateral

breast which turned out to be false-positive (figure 14). Despite the fact that not all additional lesions could be visualised at US and US-guided biopsy could thus not always be performed, the suspected lesions were removed during surgery in 19 of the 20 patients (except for the patient with a follow-up MRI of the contralateral lesion which was not detectable on US).

An example of multicentric breast cancer is shown in figure 15. This 47 year old patient presented with a palpable mass in the right breast. Mammographic and sonographic results were negative. The patient got a follow-up US 6 months later. At that moment, the sonogram demonstrated a hypo-echoic mass in the right breast measuring 4 cm. US-guided needle biopsy revealed ILA. The preoperative MRI scan also found the malignant mass in the right breast at location C9. However, the diameter was found to be larger (6.1 cm). Besides this mass, MRI identified 4 additional enhancing lesions located near the nipple. Although these additional lesions could not be seen on a second-look US and a biopsy could not be performed, the surgical plan was changed from a lumpectomy to a mastectomy because MR images showed suspicious multicentric cancer. The final pathologic result confirmed the MRI findings.

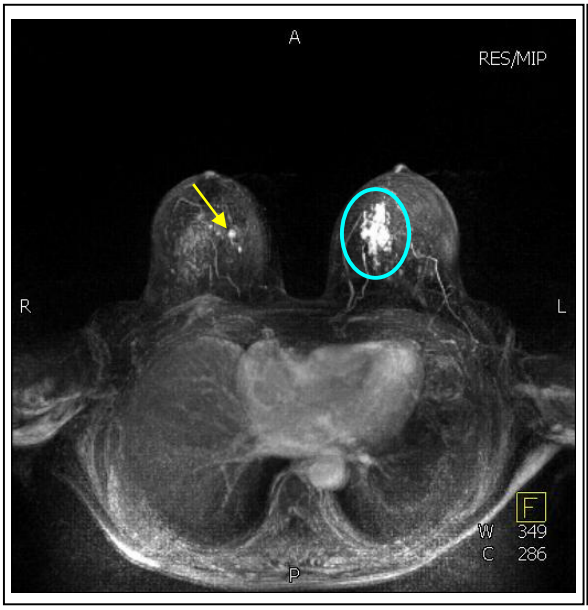

Figure 14: Example of a false-positive MRI result. This 69 year old patient has a multicentric IDA surrounded by DCIS in the left breast (blue circle). An additional lesion of approximately 5 mm was found in the contralateral breast (yellow arrow). US also detected a small hyporeflective lesion and a fine needle aspiration cytology was performed. Histopathologic examination yielded a benign intraductal papilloma.

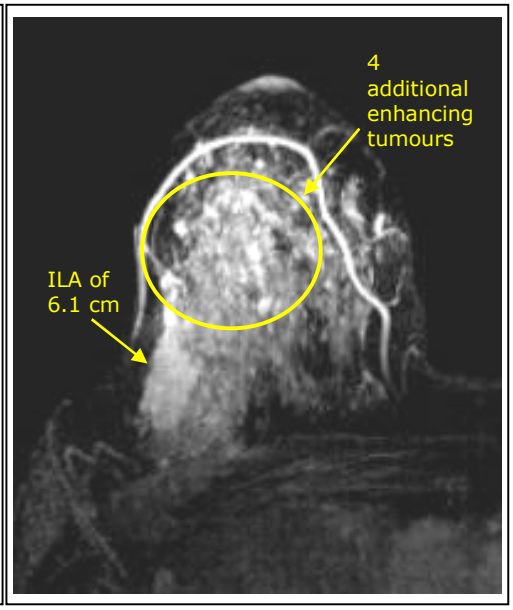

Figure 15: The right breast of a patient with multicentric breast cancer. According to US, the diameter of the tumour was 4 cm. MRI yielded a tumour size of 6.1 cm. In addition four extra enhancing lesions were found near the nipple. A mastectomy was performed and histopathology confirmed the MRI results: one big tumour of about 6 cm and four separate little tumours. In this particular case, the surgical plan was changed from breast conservation therapy to mastectomy as a result of the preoperative MRI findings.

Except for one patient whose resection specimen had been disappeared, the malignancy of the additional lesions was verified by pathologic examination. IDA + DCIS was found in 4 patients, ILA + LCIS in 1 patients, ILA in 6 patients, IDA in 7 patients, and precancerous tissue in 1 patient. In 4 of the 19 patients, the surgical plan was changed as a result of the extra findings obtained by MRI. A schematic representation of the results is shown in figure 16 (left part).

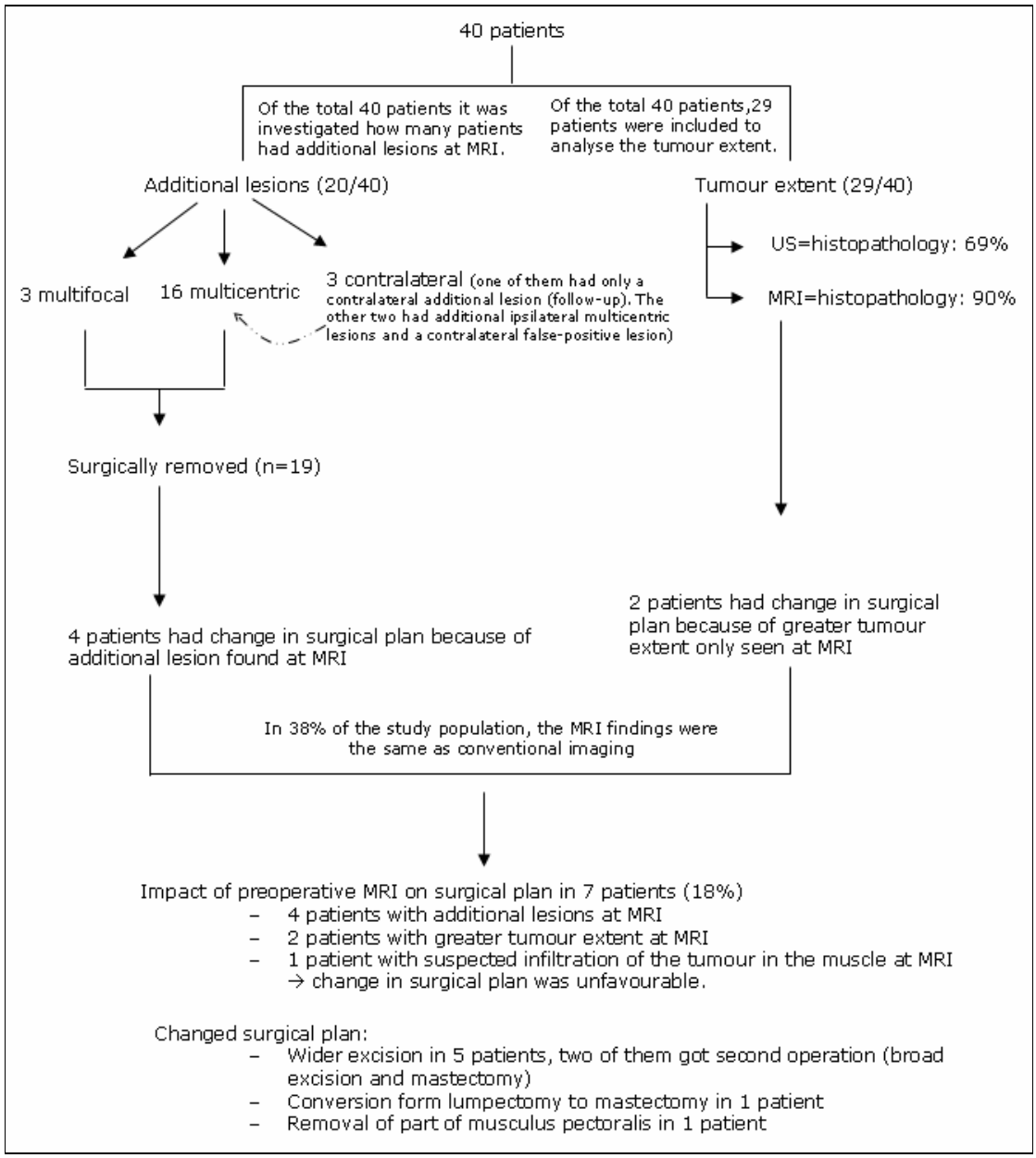

Figure 16: schematic representation of the results.

Figure 17 shows a second patient with an additional breast lesion identified at MRI. This woman found a palpable mass in the right breast. Clinical breast examination revealed a 3 cm lump in the right breast, with malignant clinical features. Mammography showed two areas of distortion of the breast tissue and the presence of a nodule. US identified two hypo-echoic lesions measuring 1.1 cm and 0.5 cm. The patient had an US-guided core needle biopsy that showed ILA. The lesion of 0.5 cm was too small to be detected at MRI. Besides the already know lesion of 1.1 cm detected at conventional imaging, MRI depicted an additional enhancing spiculated mass in the right breast, that was not visible at conventional imaging. The MRI appearance was considered suspicious for multifocal cancer, with a total diameter of 4 cm. The time-intensity curve of the additional mass had a benign appearance and the brightness of the additional lesion was lower than the intensity of the known nodule. The ADC value could not be measured because the lesion was too vague to be seen on the diffusion-weighted images. Although the lesion had only morphologic malignant characteristics and could not be found on a second-look ultrasound, a wider excision was performed than previously planned in order to remove this additional suspected lesion. Histopathologic research confirmed the presence of an additional lesion, more specifically an area of invasive cancer cells from the primary ILA. During anatomic pathologic research, one resection margin of the surgical specimen was found to contain cancer. Consequently, the patient had to undergo a second broad excision to remove the residual tumour tissue. The total diameter of the two lesions was 7.5 cm. Although MRI found the additional tumour tissue, it underestimated the tumour size in this particular case.

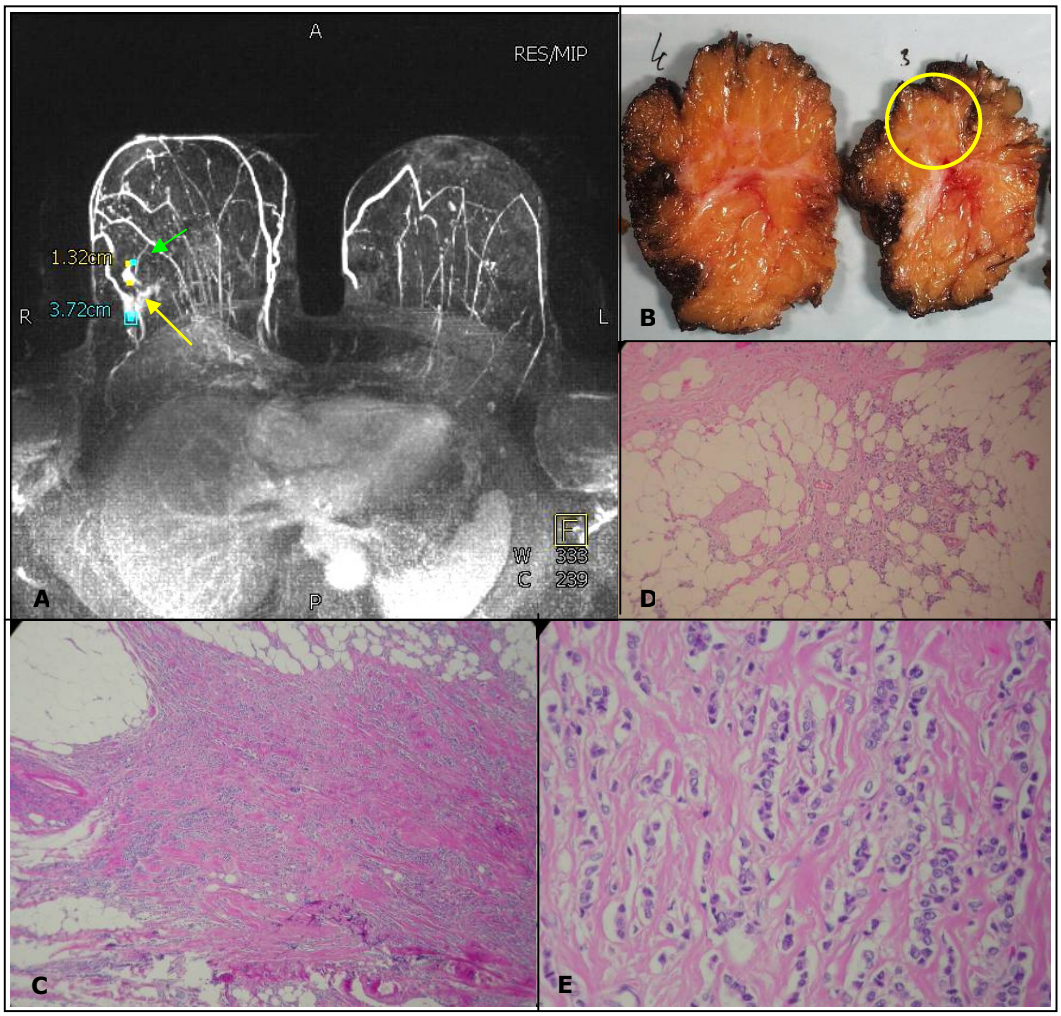

Figure 17: A 73 year old woman with a palpable nodule in the right breast. A: Mammography, US and MRI revealed a spiculated mass in the right breast (green arrow). Only MRI revealed an additional lower intense region, caudal of the first lesion (yellow arrow). B: The original tumour is present in slice 3 of the resection specimen. C: Microscopic picture of the original ILA, a dense compact area. D: The additional cancer infiltrates the fatty tissue. E: Strands of tumour cells infiltrate the stroma, in the so-called "Indian" filing pattern.

Figure 18 shows a precancerous area detected by MRI. This patient presented with a palpable mass in the right breast which was found at mammography and US. After biopsy, the mass was classified as IDA surrounded by DCIS. MRI found 2 lesions. The additional lesion was smaller than 5 mm and had a blurred surrounding enhancement. It was suspected malignant on the basis of its morphologic appearance. Because of the small size of the most intense region of the lesion, it was not possible to place a ROI, analyse the contrast enhancement curve, nor to measure the ADC-value. Even though this region could not be found by a second-look US and thus a biopsy could not be preformed, a wider excision was made to remove the additional suspected area. The final histopathologic results showed that the suspected lesion was a region of high proliferation of epithelial cells (hyperplasia). Although still benign, this breast tissue could evolve into malignant tissue.

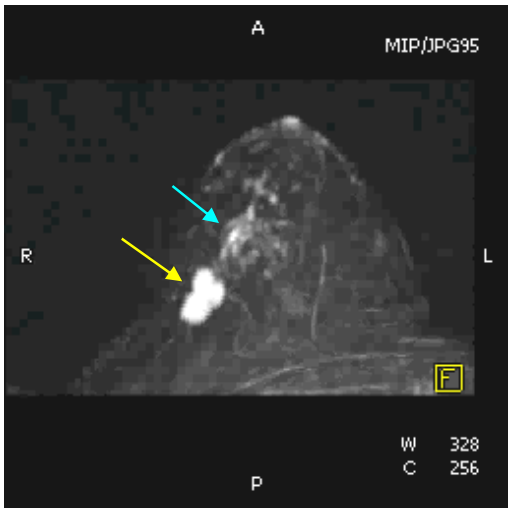

Figure 18: A 44 year old patient presented with a mass on mammography and US. This mass was also found at MRI (yellow arrow). The additional lesion (blue arrow), which was occult at conventional imaging, appeared to be precancerous tissue.

3.2.4 Tumour extent

A comparison was made between the lesion extent determined by MRI and by conventional imaging. As a reference, the histopathologic tumour extent was used. 29 patients with available US, MRI and histopathology results were included in this substudy. A size tolerance of 1 cm was used. The tumour extent measured by US, MRI and histology ranged respectively from 0.8-4.0 cm over 0.6-8.5 cm to 0.5-9.0 cm (table 1). In 69% of the cases, US findings were similar to the histopathologic measurements. MRI, however, agreed with histopathology in 90% of the cases. Neither US nor MRI overestimated the tumour size. US and MRI underestimated the tumour size respectively in 9 cases ($p<0.05$) and 3 cases (p 0.103) (one case is illustrated in figure 17).

Figure 19 shows the linear regression analyses of the comparison of the tumour diameters determined by US and MRI versus the histopathologic measurements. The correlation coefficient of US and histopathology is rather low ($R=0.43$, $p=0.019$). MRI correlates very well with histopathology ($R=0.93$). There is a significant linear correlation between the two variables MRI and histopathology ($p<0.05$).

Table 1: Comparison between the lesion extent determined by MRI, US and histopathology.

Imaging technique	Size range (cm)	Deviation to histopathologic size cm ± SD*	p
US	0.8-4.0	-1.16 ± 2.04	0.005
MRI	0.6-8.5	-0.27 ± 0.86	0.103
Histology	0.5-9.0		

*Standard deviation

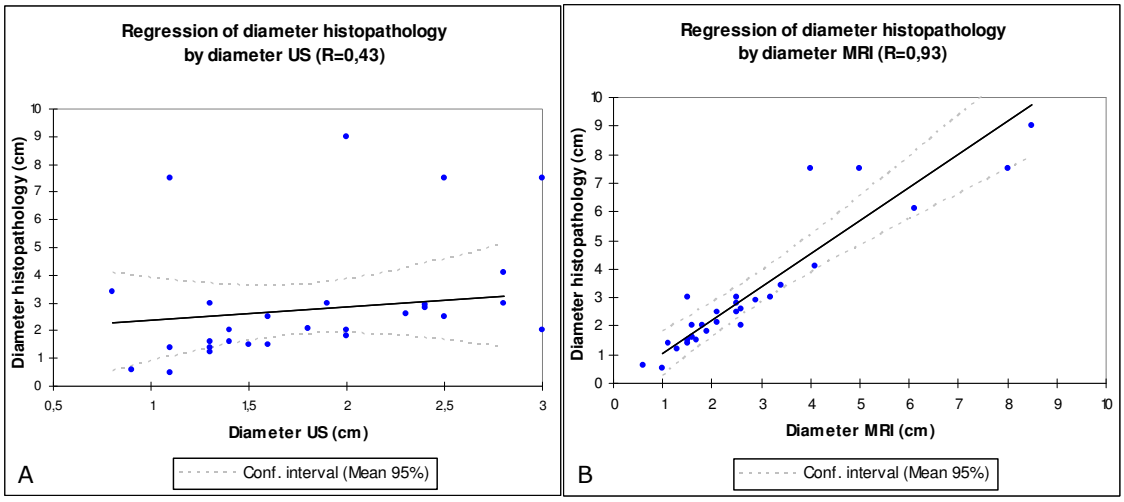

Figure 19: A: Correlation of total lesion diameter (in cm) measured by US and by histopathology. B: Correlation of total lesion diameter measured by MRI and by histopathology.

In 7% of the patients (2/29) the surgical plan was changed. A wider excision was performed based on the larger tumour extent seen at MRI in comparison to US (see figure 16 for a schematic representation of these results (right part)). The tumour extent was later confirmed by histopathology.

Figure 20 is an illustration of a larger tumour extent detected by MRI. This 50 year old women presented with a palpable mass in the right breast. Clinical breast examination revealed a 2.5 x 3.5 cm lump in the right breast with malignant clinical features. US identified an irregular hypo-echoic lesion with a diameter of 2.8 cm. An ultrasound-guided core biopsy was performed and histopathologic examination revealed IDA. At MRI, the tumour had a caudal extension, yielding a maximal tumour diameter of 4.1 cm. The patient got a wider excision than originally planned. Histopathology of the resection specimen revealed IDA, associated with DCIS. The extension of the tumour turned out to be highly proliferative epithelial cells (hyperplasia) which later on can develop into malignant tissue.

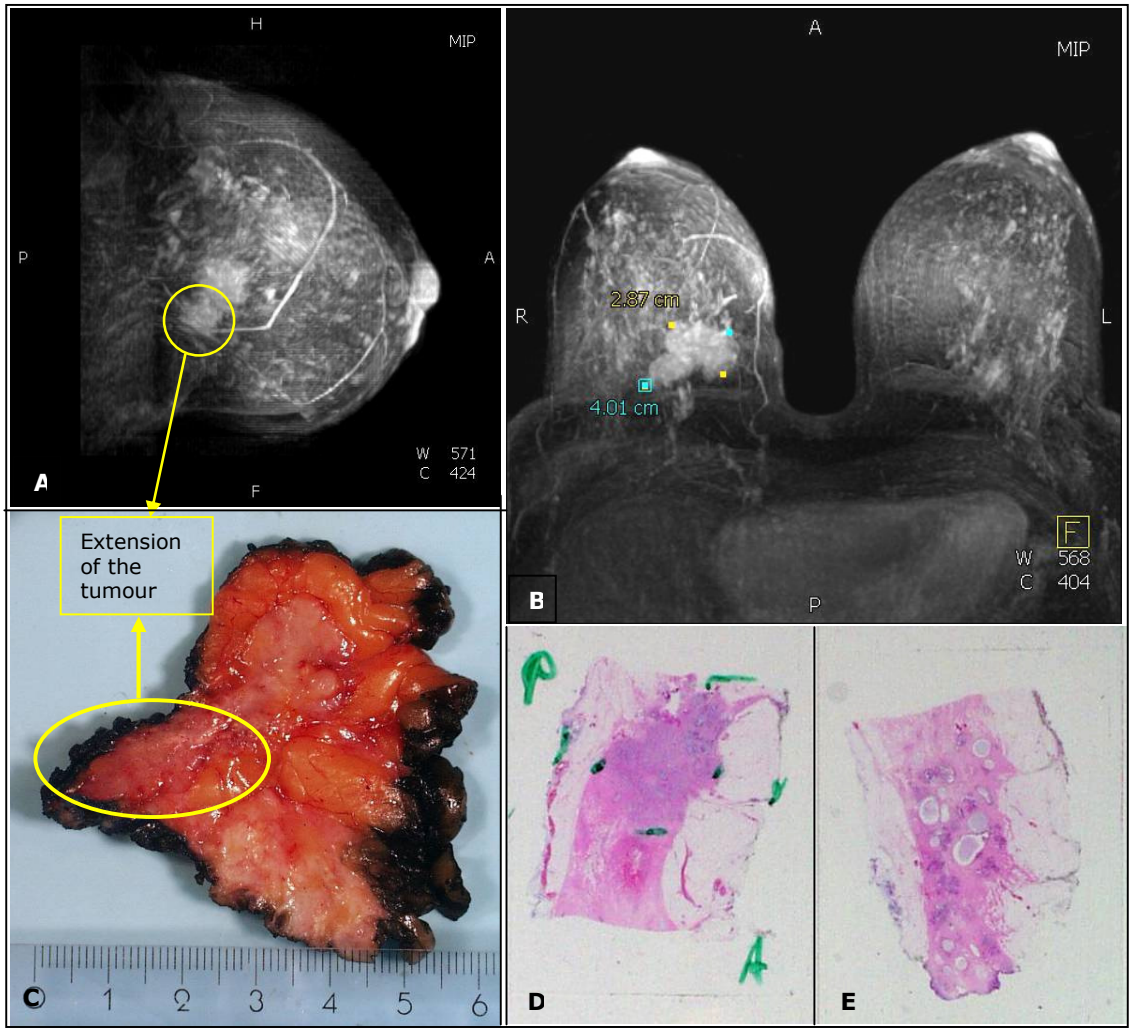

Figure 20: A 50 year old woman with IDA associated with DCIS in the right breast. At MRI, the tumour had a caudal extension (A) with a maximal diameter of 4.1 cm (B). The extension was clearly visible on the resection specimen (C). After histochemical staining, the tumour could be microscopically visualised as a compact mass (D). The extension contains highly proliferative tissue and is characterised by dilation of the ducts (E).

3.3 Impact of preoperative MRI on the surgical plan

The effect of preoperative breast MRI on the surgical management of the patients is shown in figure 16 and figure 21. Among the total study population (40 patients), preoperative MRI findings changed the surgical plan of 7 patients (18%). In four patients additional lesions were found, in two patients a larger tumour size was determined. In one patient tumour infiltration in the pectoralis muscle was suspected (figure 22).

In 5 patients the planned broad excision was replaced by a wider excision. In 1 patient there was a conversion from lumpectomy to mastectomy. A part of the pectoralis muscle was removed in one patient in addition to the planned mastectomy (table 2).

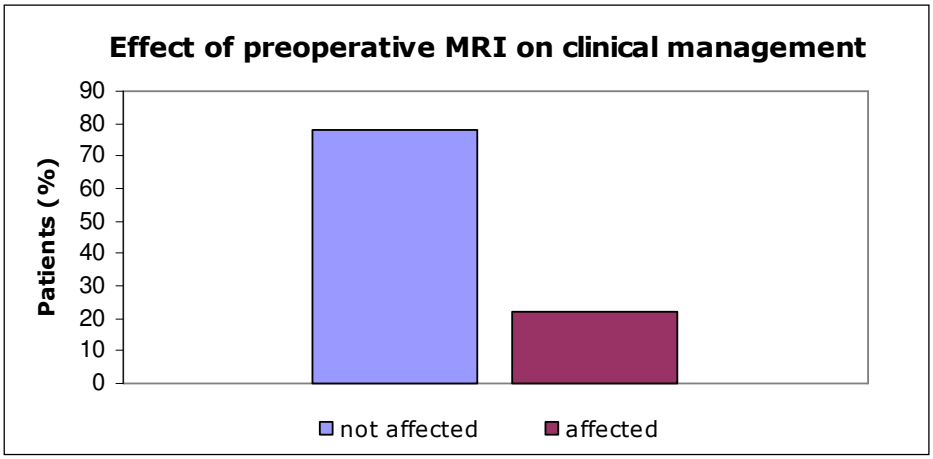

Figure 21: Effect of preoperative MRI on the clinical management of women with proven breast cancer.

Table 2: Patients for which the surgical plan was changed because of MRI findings.

Patient	Histology	MRI findings	Operation planned	Operation performed
1	IDA (additional lesion not known)	Greater tumour size	BE*	Wider excision
2 (fig.18)	IDA + DCIS	Additional lesions	BE	Wider excision
3 (fig.20)	IDA + DCIS	Greater tumour size	BE	Wider excision
4	IDA + DCIS	Additional lesions	BE	Wider excision + ME
5 (fig.17)	ILA + LCIS	Additional lesions	BE	Winder excision + second BE
6 (fig.22)	IDA	Tumour suspected for infiltration in muscle	ME**	ME + part of the muscle
7 (fig.15)	ILA	Additional lesions	BE	ME

*BE= broad excision (tumourectomy), **ME= mastectomy.

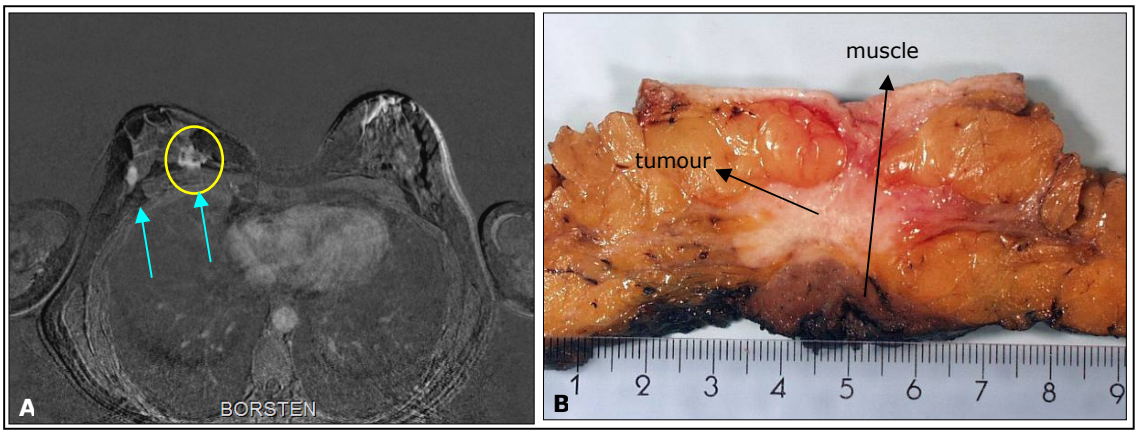

Figure 22: A 52 year old woman with 2 tumours in the right breast (IDA) (arrows). On the MR image it seems that one tumour infiltrates the pectoralis muscle (yellow circle) (A). Therefore, a part of the muscle was removed during mastectomy. However, histopathologic research did not found any tumour cells in the muscle. The tumour is located at a distance of 8 mm of the muscle (B).

Figure 23 show the resection specimen of a patient who did not get a preoperative MRI scan. Mammography and ultrasonography detected a mass in the right breast. Analysis of biopsy specimen revealed IDA. A broad excision was performed to remove the cancer. Histopathologic research of this specimen found a second tumour (IDA + DCIS). The resection specimen contained positive margins. Consequently, a second operation (broad excision) was needed to remove the residual cancerous tissue. A preoperative MRI would possibly have avoided the need for a second surgical intervention.

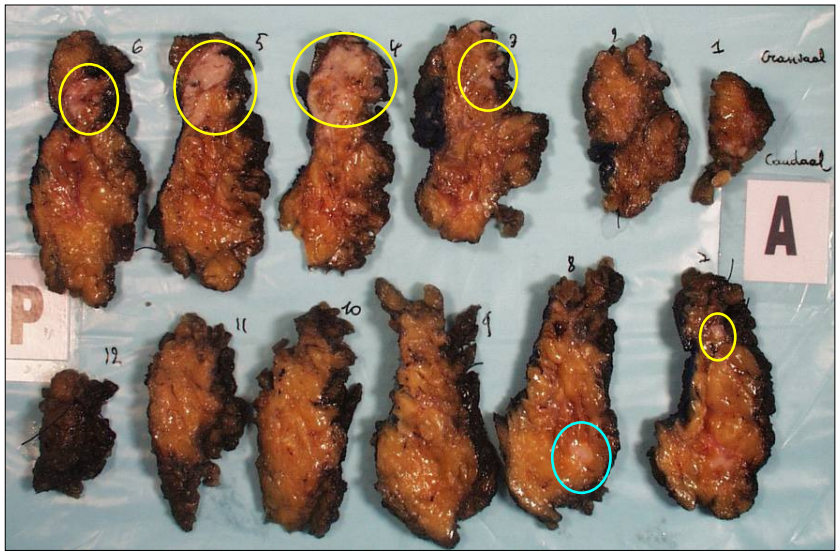

Figure 23: Resection specimen of a 70 year old patient who underwent a lumpectomy because conventional imaging and biopsy found a tumour in the right breast (blue circle, slice 8). Final histopathologic research of the specimen found a second tumour in slice 3-7, extended to the cranial and anterior margins (yellow circles). The second tumour was not seen at conventional imaging.

4 Discussion

Today, most malignant breast tumours are treated with breast conservation surgery. Complete tumour removal is mandatory in order to avoid recurrence. Therefore, exact preoperative information about the size, extent and location of the tumour is necessary [34]. According to several studies, MRI has a high sensitivity (89-100%) for the detection of breast cancer [28]. It has been used as an adjunct to mammography for patients with equivocal mammographic and sonographic findings, as well as for several other indications such as evaluation of breast implants, evaluation of neoadjuvant chemotherapy, or follow-up of high risk patients. It can never replace mammography as a first-line examination. The impact of routine MRI on the surgical management of new biopsy proven breast cancers, however, remains unclear.

Studies have shown that MRI has a variable specificity (37-97%) in detecting malignant breast lesions [35]. Enhancing lesions are not per definition malignant but can also can be benign (e.g. fibroadenomas, galactitis). Moreover, even normal breast parenchyma may enhance in the presence of hormonal stimulation. Particularly in young patients (hormonally active women), spontaneous contrast-enhancing foci may occur, corresponding to the breast's physiological response to cyclical hormonal stimuli. The effect of the menstrual cycle on contrast enhancement is lowest in week 2 and highest in week 1 and 4. For this reason, MRI is best performed during the second week of the menstrual cycle, to avoid enhancement of normal tissue. Hormone replacement therapy can also induce false-positive results, so a MRI scan should be performed two or three months after therapy interruption [36]. An increased angiogenic activity is not only found in malignant tissue, but also in inflamed tissue and during the process of wound-healing [28]. For this reason, MRI will never replace mammography or ultrasonography as a screening test for breast cancer, it will rather be used as an additional/complementary test. The decision of performing a preoperative MRI scan should be based on the findings of conventional imaging methods. Mammography and US yield information about the location of the lesion and biopsy rules out whether or not the lesion is malignant. A preoperative MRI scan might yield a more precise description about the location, size, multifocality or multicentricity of the tumour and might detect possible additional tumours. This information may in turn alter the staging of the disease and lead to a change in the treatment planning.

An overview of the patients included in this study is given in appendix 2 and 3. Note that patients with a well-differentiated tumour had a higher incidence of lymph node metastases. This is in contrast to the literature which states that well-differentiated (grade 1) tumours have a lower incidence of nodal positivity [37]. The fact that only women with a biopsy proven breast cancer were studied, explains the high sensitivity of mammography (87%) and ultrasonography (97%) in this study, as well as the low number of MRI false-positive results.

MRI has a variable specificity because benign changes and normal breast tissue may enhance too [28]. For this reason, several studies concluded that MRI may not be used for every women to screen the breasts for the detection of possible breast lesions. That is why most institutions use several indications for performing breast MRI. The difference of our study compared to many other studies is that we used a population of women that already have a proven breast cancer.

Although MRI has a high sensitivity in detecting breast tumours, there were 3 false-negative results in our study. There are several reasons why these tumours were not seen at MRI. One explanation is the 5 mm threshold for the detection of tumours at MRI. Tumours of 5 mm or smaller are hard to detect at MRI [38]. Small lesions are also hard to distinguish from the surrounding parenchyma because of diffuse enhancement in a premenopausal patient. A second explanation is haemorrhage resulting from biopsy. A haemorrhagic region already enhances on precontrast images resulting in a black lesion on the subtraction image. In addition, core biopsy may reduce the diameter of the tumour to a size below the 5 mm threshold. A third cause of missed lesions at MRI is the movement of the patient during the dynamic series. The position of the lesion on the precontrast image differs from the position of the lesion on the postcontrast images. Subsequently, after subtraction of the precontrast image of the postcontrast image, there will be no enhancement in the region where the lesion is situated. There were 2 false-positive result (figure 14). In these cases, biopsy was not necessary because the lesion turned out to be benign. To reduce the number of false-positive results, additional enhancing foci smaller than 5 mm should be ignored.

In order to achieve optimal discrimination between benign and malignant lesions found at MRI, both kinetic and morphologic information is required [39]. In this study, in 8 (20%) patients the contrast-captation curves were found to be aspecific and inconclusive. Some malignant lesions showed a type I curve (benign) and other malignant lesions showed inconclusive curves. In order to increase the specificity of breast MRI, DWI was performed [40]. Brownian motion is the free random movement (diffusion) of molecules as a result of thermal fluctuations. The motion of water molecules is restricted by the presence of cell membranes, vascular structures and macromolecules [4]. This results in a lower apparent diffusion coefficient (ADC) value, which is the net displacement of water molecules. The diffusion coefficient varies between tissues and may be altered due to pathology. As malignant lesions have a higher cellularity than normal fibroglandular tissue, the ADC value will be lower, allowing differentiation between malignant and normal tissue. Benign lesions contain more free water and yield higher ADC values [41]. It is worthwhile to note that the threshold ADC value for differentiating between benign and malignant breast tissue is not known. Different authors use different ADC levels as a threshold for diagnosing breast cancer (appendix 4), with an average threshold ADC value of 1.31×10^{-3} mm^2/s [41].

Our findings show a remarkable better correlation between DWI and tumour malignancy than between time-intensity curves and tumour malignancy. The ADC values of most benign tumours were higher than those of malignant tumours (figure 10). The ADC values of malignant tumours ranged mainly between 0.7 and 1.3 x 10^{-3} mm^2/s. However, there were also some exceptional high ADC values. This can be due to central tumour necrosis [31]. A high ADC value can also be related to a small tumour size (< 1 cm). It is clear that more patients have to be included in order to find a threshold ADC value and to incorporate these measurements into the BI-RADS classification. Despite the promising results of DWI, it should not replace contrast-enhanced imaging, since small breast lesions (<1 cm) are often hard to visualize on the DWI and may yield wrong ADC values. These lesions therefore should better not be evaluated with DWI [41,42]. Instead, DWI can be used as a complementary tool to the contrast capitation kinetics.

In this study, preoperative MRI detected additional unsuspected tumour areas in 20 (50%) breast cancer patients (see section 3.2.3). In most patients these lesions were not found on the second-look US, making a biopsy impossible. Nevertheless, the additional lesions were removed in all but one patient. In this patient, a follow-up MRI was planned which mostly takes place 6 to 8 weeks later. In the other patients in which the additional tumour was removed during surgery, the histopathologic results demonstrated malignancy (except for one patient of which the resection specimen was lost). The lesions not found on the second-look US were infiltrating ILA (figure 17) and precancerous tissue (figure 18). Lobular cancer is one of the most frequently missed cancers by mammography and ultrasonography. The reason for this is that the infiltrating cells form columns of cells (the "Indian" filing pattern) rather than forming discrete masses or easy detectable distortion. Therefore, they are hard to detect at US. However, MRI does not detect masses but it detects contrast enhancement. Because of its diffuse infiltrative nature, ILA is a common indication to perform MRI [43,35,1]. Pre-cancerous tissue (hyperplasia) could also not be seen as a dense mass at US. Without a MRI scan, these lesions would possibly have remained undetected, resulting in recurrence of breast cancer and possibly in a worse prognosis.

In the future, the Department of Radiology will invest in a specialized breast coil allowing MRI-guided biopsy. Kuhl et al (2007) stated that "preoperative MRI should only be offered by institutions that can offer MRI-guided biopsy of the additional lesions or of the additional extent of a known cancer" [44]. In our study population there were several cases in which additional lesions found at MRI could not be found at US, so a biopsy could not be performed. With the help of MRI-guided biopsy, there would be definite prove of malignancy of the additional lesions or the additional extent of a known tumour found at MRI. In turn, this might reduce the anxiety of the patients, who otherwise would get a follow-up scan several months later, as well as the doubt of the radiologists and surgeons to remove suspected additional lesions.

Accurate preoperative size assessment of a malignant breast tumour is not only important for staging of the tumour but also for treatment planning. It is important in preoperative evaluation as breast-conserving surgery is frequently replacing mastectomies. Complete tumour removal is necessary to avoid recurrence of the cancer. Tumour borders may be poorly demarcated on mammography, especially in dense breasts [34]. In this study, (section 3.2.4), US and MRI tumour extent measurements were compared with the histopathological results, allowing a 1 cm deviation. 29 of the total 40 patients were included to analyse the tumour extent. While US underestimated the extent of the tumour in 9 patients, this only occurred three times in the case of MRI. Neither technique overestimated the tumour extent. MRI results correlated more accurately with histopathological findings ($R=0.93$, $p<0.05$) than US did ($R=0.43$, $p=0.019$) (figure 19). MRI seems to be a more accurate imaging technique compared to conventional imaging.

The number of patients whose treatment was changed because of the preoperative MRI findings was relatively high (18%) (figure 21). 4 patients had additional breast lesions that were occult on conventional imaging, while 2 patients had a larger tumour extent measured at MRI. In one patient, the tumour at MRI was suspected to infiltrate the pectoralis muscle. The remaining patients (82%) had no treatment-relevant additional information revealed at MRI or already had an optimal treatment plan, like mastectomy or neoadjuvant chemotherapy, based on conventional imaging. One could question whether a change in the surgical plan is really necessary. Opponents argue that breast MRI may lead to overdiagnosis and overtreatment, when additional breast cancers are found that do not threat a woman's survival [44]. For instance, figure 18 shows an additional lesion found at MRI that was surgically removed. This lesion appeared to consist of highly proliferative tissue (hyperplasia). The radiation therapy usually given after a breast-conservation therapy might have destroyed this high-risk tissue and a broader excision might thus not have been necessary [44]. Is it therefore justified to not remove this enhancing area seen at MRI? Do all patient benefit from the changed surgical plan? In order to find an answer to such questions, it has to be known how much residual disease in the breast can be controlled with radiation. The easiest way to investigate this, is a case-control study in which the control group consists of patients with proven breast cancer that do not get a preoperative MRI scan. In this way, the recurrence rate after breast conservation therapy can be compared within these two groups. Obviously, such a study is not ethical acceptable.

The patient population in this study is rather small. A larger prospective study is needed to evaluate the benefit of preoperative breast MRI. No studies have yet demonstrated if the change in management resulting from additional information obtained by MRI is ultimately beneficial for the patient in terms of decreasing overall mortality. Patients will be monitored for several years to measure their overall survival rate, compared with that of patients from

the past who did not get a preoperative MRI scan. We will determine whether preoperative MRI is able to reduce the frequency of cancer recurrence in the treated breast and whether it yields a better life-expectancy.

5 Conclusion

There is still a great deal of uncertainty about the role of MRI in breast cancer detection. The purpose of this study was to evaluate the added therapeutic value of preoperative MRI in patients with a biopsy proven breast cancer. Preoperative MRI may gain additional information about location and extent of breast cancer. Because of its accuracy, the additional information provided by MRI may in turn affect the tumour staging and the surgical plan of the patient.

Over a period of several months, women with biopsy proven breast cancer were evaluated with an additional preoperative MRI scan. Simultaneously, DWI was evaluated and optimized. Although routinely used in MR imaging of the brain, DWI is not yet a standard procedure in MR imaging of the breast.

In comparison to conventional imaging techniques, MRI was found to be more accurate in assessing the extent of breast cancer and in detecting additional lesions. In 18% of the patients, MRI findings led to a change in the surgical plan. In 71% of the patients with additional MRI findings, histology confirmed its malignancy. Whereas the contrast-captation (time-intensity) curves were found to be mainly aspecific and inconclusive, DWI seems to show great promise in differentiating between benign and malignant lesions and will therefore be routinely performed in the future in our department. The MR images also help the pathologist to analyse the surgical resection specimen. The reconstruction of three-dimensional images, clearly showing the location and extent of the lesions, was positively scored by the surgeon and the pathologist.

While the majority of published data about breast MRI has been favourable, it has not been enthusiastically embraced. MRI is not yet a standard method for evaluation of breast tumours. Currently, its low specificity had been cited as a barrier to breast MRI use in clinical practice. Other disadvantages of MRI are its high costs, the limited availability of MRI-guided biopsy, and the lack of uniformity in technique and image interpretation among different institutions [45-46]. Standardization is needed to generalize novel findings to other institutions. A standardized application combined with MRI-guided biopsy will allow a more precise characterization of known and additional lesions. This might prevent incomplete surgeries and reduce tumour recurrence, ultimately reducing the overall costs associated with breast cancer. A larger study population, including a life-expectancy evaluation over a longer period of time as well as a cost-effective analysis, is needed to define whether every women with proven breast cancer should get a preoperative MRI scan in the future.

6 References

1. Mallon E, Osin P, Nasiri N, et al. The basic pathology of human breast cancer. Journal of mammary gland biology and neoplasia 2000;5:139-163.
2. Tyczynski JE, Bray F, Parkin DM. Breast cancer in Europe. European network of cancer registries 2002;2:1-4.
3. Belgian cancer registry. URL: www.kankerregister.org
4. Blackwell RE, Grotting JC. Diagnosis and management of breast disease. Grotting: Blackwell science; 1996.
5. Robbins SL, Cotran RS, Kumar V. Breast. Basic pathology 7th edition. China: Saunders Elsevier; 2003: p.705-718.
6. Orel S. Society of breast imaging. Applications and interpretation of breast MRI. Lecture: indications for MR imaging of the breast. Boston, Massachusetts: The American college of radiology; 2008.
7. Boyce JD. Sprecher institute for comparative cancer research. Ionizing radiation and breast cancer risk, 2005.
   URL: http://envirocancer.cornell.edu/factsheet/physical/fs52.radiation.cfm
8. Stevens A, Lowe J. Huid en borsten. Histologie van de mens. Bohn Stafleu van Loghum; 1998. p. 355-375.
9. Rubin E, Farber JL. Pathology. Chapter 19 The breast. Philadelphia: Lippincott JB company; 1988. p. 990-1013.
10. Sternberg SS. Chapter 9 The breast. Diagnostic surgical pathology volume 1. Third edition. Philadelphia: Lippincott Williams and Wilkins; 1999. p. 319-385.
11. Catalogus breast imaging reporting and data system (bi-rads). American college of radiology.
12. Macéa JR, Fregnani JH. Anatomy of the thoracic wall, axilla and breast. International journal of morphology 2006;24:691-704.
13. Stahl J. Gynaecological pathology. Revision of breast anatomy, and lymph drainage 2004. URL: http://cal.fmc.flinders.edu.au/gemp/ClinicalSkills/clinskil/year2/breast/breast01.htm
14. Dr. S Love research foundation. Breast cancer, 2009. URL: http://www.dslrf.org/breastcancer/content.asp?L2=1&L3=1&SID=120
15. Heywang-Köbrunner SH, Dershaw DD, Schreer I. Diagnostic breast imaging. Mammography, sonography, magnetic resonance imaging, and interventional procedures, second edition. New York: Thieme; 2001.
16. Osako T, Iwase T, Takahashi K, et al. Diagnostic mammography and ultrasonography for palpable and nonpalpable breast cancer in women aged 30 to 39 years. Breast Cancer 2007;14:255-259.
17. Kolb TM, Lichy J, Newhouse JH. Comparison of the performance of screening mammography, physical examination, and breast US and evaluation of factors that influence them: an analysis of 27,825 patient evaluations. Radiology 2002;225:165-175.
18. Lord SJ, Lei W, Craft P, et al. A systemic review of the effectiveness of magnetic resonance imaging (MRI) as an addition to mammography and ultrasound in screening young women at high risk of breast cancer. European journal of cancer 2007:1905-1917.
19. Fornage BD. Sonographically guided needle biopsy of nonpalpable breast lesions. Journal of clinical ultrasound 1999;27:385-398.
20. Helbich TH, Matzek W, Fuchsjäger MH. Stereotactic and ultrasound-guided breast biopsy. European radiology 2004;14:383-393.

21. Schmidt RA. Stereotactic breast biopsy. CA a cancer journal for clinicians 1994;44:172-191.
22. MRI-guided breast biopsy, 2008. The American college of radiology and the radiological society of North America. URL: www.radiologyinfo.org.
23. Sainsbury JRC, Anderson TJ, Morgan DAL. Breast cancer. ABC of breast diseases. Clinical review. BMJ 2000;321:745-751.
24. Collins CD. The sentinel node in breast cancer: an update. Cancer imaging 2005;5:3-9.
25. Holmes CE, Muss HB. Diagnosis and treatment of breast cancer in the elderly. CA a cancer journal for clinicians 2003;53:227-244.
26. Westbrook C, Roth CK, Talbot, J. MRI in practice, third edition. USA: Blackwell publishing; 2005.
27. Roberts PA, Williams J. Farr's physics for medical imaging, second edition. UK: Saunders, Elsevier; 2007.
28. Kuhl C. The current status of breast MR imaging. Part I. Choice of technique, image interpretation, diagnostic accuracy, and transfer to clinical practice. Radiology 2007;244:356-378.
29. Orel SG, Schnall MD. MR imaging of the breast for the detection, diagnosis, and staging of breast cancer. Radiology 2001;220:13-30.
30. DeMartini W, Lehman C. A review of current evidence-based clinical applications for breast magnetic resonance imaging. Topics in magnetic resonance imaging 2008;19:143-150.
31. Wenkel E, Geppert C, Uder M, et al. Diffusion-weighted imaging in breast MRI – An easy way to improve specificity. Clinical women's health. Magnetom flash 2007:28-32.
32. Jiang ZX, Peng WJ, Li WT, et al. Effect of b value on monitoring therapeutic response by diffusion-weighted imaging. World journal of gastroenterology 2008;14:5893-5899.
33. Tozaki M. Interpretation of breast MRI: Correlation of kinetic and morphological parameters with pathological findings. Magnetic resonance in medical sciences 2004;3:189-197.
34. Hlawatsch A, Teifke A, Schmidt M, et al. Preoperative assessment of breast cancer: sonography versus MR imaging. American journal of roentgenology 2002;179:1493-1501.
35. Van Goethem M, Verslegers I, Biltjes I, et al. MR is/is not a useful diagnostic tool for breast cancer management. Acta chirurgica belgica 2007;107:267-270.
36. Van Goethem M, Tjalma W, Schelfout K, et al. Magnetic resonance imaging in breast cancer. European journal of surgical oncology, Elsevier 2006;32:901-910.
37. Arisio R, Sapino A, Cassoni P, et al. What modifies the relation between tumour size and lymph node metastasis in T1 breast carcinomas? Journal of clinical pathology 2000;53:846-850.
38. Kelcz F, Furman-Haran E, Grobgeld D, et al. Clinical testing of high-spatial-resolution parametric contrast-enhanced MR imaging of the breast. American journal of roentgenology 2002;179:1485-1492.
39. Orel SG. Differentiating benign form malignant enhancing lesions identified at MR imaging of the breast: Are time-signal intensity curves an accurate predictor? Radiology 1999;211:5-7.
40. Marini C, Iacconi C, Giannelli M et al. Quantitative diffusion-weighted MR imaging in the differential diagnosis of breast lesion. European radiology 2007;17:2646-2655.
41. Park MJ, Cha ES, Kang BJ, et al. The role of diffusion-weighted imaging and the apparent diffusion coefficient (ADC) values for breast tumors. Korean journal of radiology 2007;8:390-396.
42. Partridge SC. Future applications and innovations of clinical breast magnetic resonance imaging. Topics in magnetic resonance imaging 2008;19:171-176.
43. Esserman L, Wolverton D, Hylton N. Magnetic resonance imaging for primary breast cancer management: current role and new applications. Endocrine-related cancer 2002;9:141-153.

44. Kuhl C, Kuhn W, Braun M, et al. Pre-operative staging of breast cancer with breast MRI: one step forward, two steps back? The breast 2007;16:34-44.
45. Lalonde L, David J, Trop I. Magnetic resonance imaging of the breast: current indications. Canadian association of radiologists journal 2005;56:301-308.
46. Tillman GF, Orel SG, Schnall MD, et al. Effect of breast magnetic resonance imaging on the clinical management of women with early-stage breast carcinoma. Journal of clinical oncology 2002;20:3413-3423.

Appendix 1: Quadrants of the breast

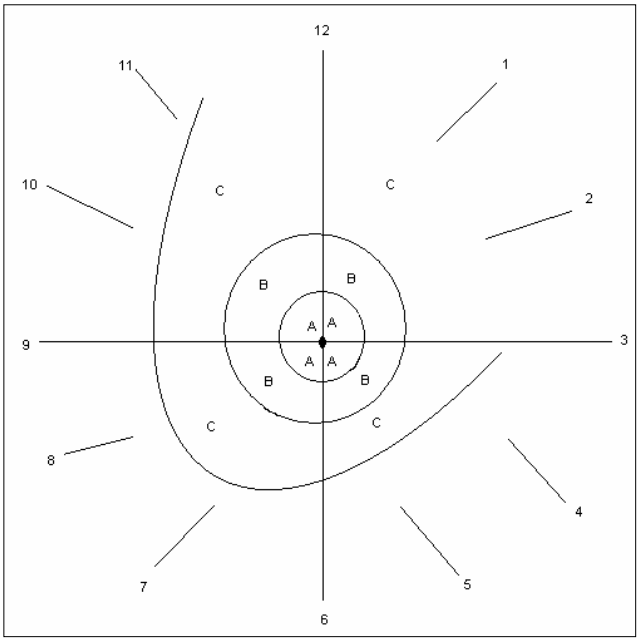

Appendix 2: Overview of patients included in the study

Patient	Age (years)	Complaints/ Symptoms	Location	Diagnosis	Surgery
1	63	Palpable mass	Left	ILA	ME* + AC**
2	69	Palpable mass	Left	IDA + DCIS	ME + AC
3	69	Screening	Left	ILA	ME
4	69	Palpable mass	Left	IDA	BE***
5	39	Palpable mass	Right	IDA	BE + AC
6	63	Screening	Right	IDA + DCIS	BE
7	44	Palpable mass	Right	IDA + DCIS	BE
8	45	Palpable mass	Right	ILA + LCIS + DCIS	BE
9	65	Screening	Right	IDA + DCIS	BE
10	69	Palpable mass	Right	IDA	BE + AC
11	50	Palpable mass	Right	IDA + DCIS	BE
12	64	Screening	Left	IDA + DCIS	BE
13	64	Pain	Right	IDA mastitis carcinomatosa	/
14	32	Pain	Left	IDA + DCIS	ME + AC
15	62	Screening	Right	IDA	BE
16	50	Palpable mass	Left	IDA mastitis carcinomatosa	ME + AC
17	56	Palpable mass	Right	IDA + DCIS	BE + ME
18	54	Screening	Left	IDA + DCIS	BE + AC
19	73	Palpable mass	Right	ILA	BE + BE
20	83	Palpable mass	Left	IDA + DCIS	ME + AC
21	52	Screening	Right	IDA	ME + AC
22	47	Palpable mass	Right	ILA	ME + AC
23	81	Palpable mass	Right	ILA mastitis carcinomatosa	/
24	55	Screening	Left	IDA + DCIS	BE + AC
25	59	Screening	Left	IDA	BE + AC
26	44	Palpable mass	Left	ILA	ME + AC
27	65	screening	Right	IDA	BE + AC
28	53	Palpable mass	Right	IDA	/

29	29	Palpable mass	Left	IDA	ME + AC
30	50	Palpable mass	Right	IDA + DCIS	BE
31	49	Screening	Right	ILA + LCIS	/
32	50	Palpable mass	Right	IDA	/
33	80	Palpable mass	Left	IDA	ME
34	50	Screening	Right	IDA	BE + AC
35	45	Palpable mass	Left	IDA + DCIS	BE
36	80	Palpable mass	Right	IDA	ME + AC
37	48	Palpable mass	Left	ILA	/
38	54	Palpable mass	Right	IDA + DCIS	BE
39	58	Palpable mass	Left	IDA	/
40	45	Palpable mass	Right	IDA + DCIS	/

*ME= mastectomy, **AC= axillary clearance, ***BE= broad excision (lumpectomy).
Patients of which the tumour was not yet surgically removed underwent neoadjuvant chemotherapy.

Appendix 3: Relation between lymph node positivity and tumour size, grade, and amount of tumours

Tumour size	**Patients (n=32)***	**Patients with positive lymph nodes**
pT1mic	1	1 (1%)
pT1a	1	0 (0%)
pT1b	4	0 (0%)
pT1c	10	4 (40%)
pT2	12	5 (42%)
pT3	4	2 (50%)
Differentiation grade	**Patients (n=31)*°**	**Patients with positive lymph nodes**
Grade 3	12	3 (25%)
Grade 2	15	7 (47%)
Grade 1	4	2 (50%)
Amount of tumours	**Patients (n=32)***	**Patients with positive lymph nodes**
Unifocal	21	5 (24%)
Multiple	11	7 (64%)

*Patients undergoing neoadjuvant chemotherapy were not included in the calculation. °The differentiation grade of one patient was not known.

Appendix 4: Overview of ADC threshold values reported in literature for breast cancer

Author, year	**ADC threshold (x 10^{-3} mm^2/s)**	**Sensitivity**	**Specificity**
Rubesova, 2005	1,20	81%	93%
Hatakenaka 2008	1,48	38,9%	81,3%
Guo, 2002	1,30	93%	88%
Wenkel 2007	1,26	/	/
Woodhams, 2005	1,60	93%	46%
Marini, 2007	1,10	80%	81%
Marini, 2007	1,31	100%	67%
Hatakenaka 2008	1,30	93%	88%
Luo, 2007	1,22	88,9%	87,9%